"G-Pisa" Ring Laser Gyroscope: Present and Future Activity

Jacopo Belfi

Department of Physics, University of Pisa, Italy

3rd International Working Group on Rotational Seismology
22-25 September 2013
University of Canterbury, Christchurch, New Zealand

Outline

Part1

Brief History of G-Pisa

Applications to seismology

Part2

The GINGER test of GR

Geometry control

Laser dynamics corrections

Why "G-Pisa"?

2008 Virgo GW-Interferometer need:
control ground rotations in the microseimic frequency region

Acceleration or rotation?

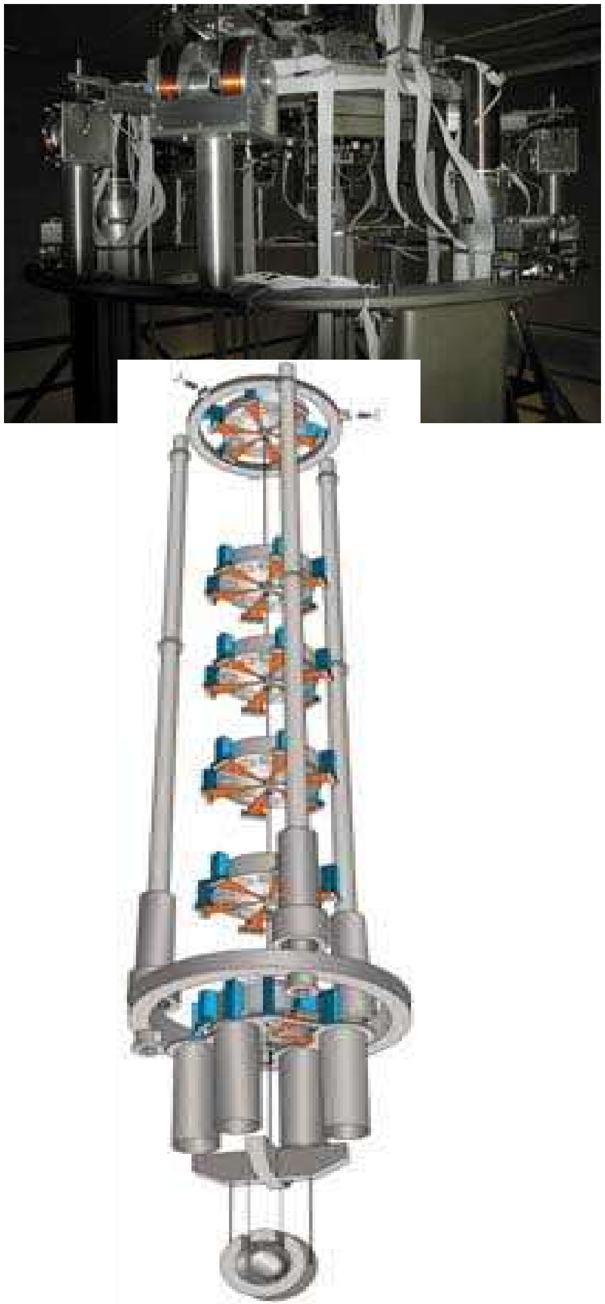

Active control of 4 d.o.f. of the IP
The two tilts around the Interferometer arms are missing

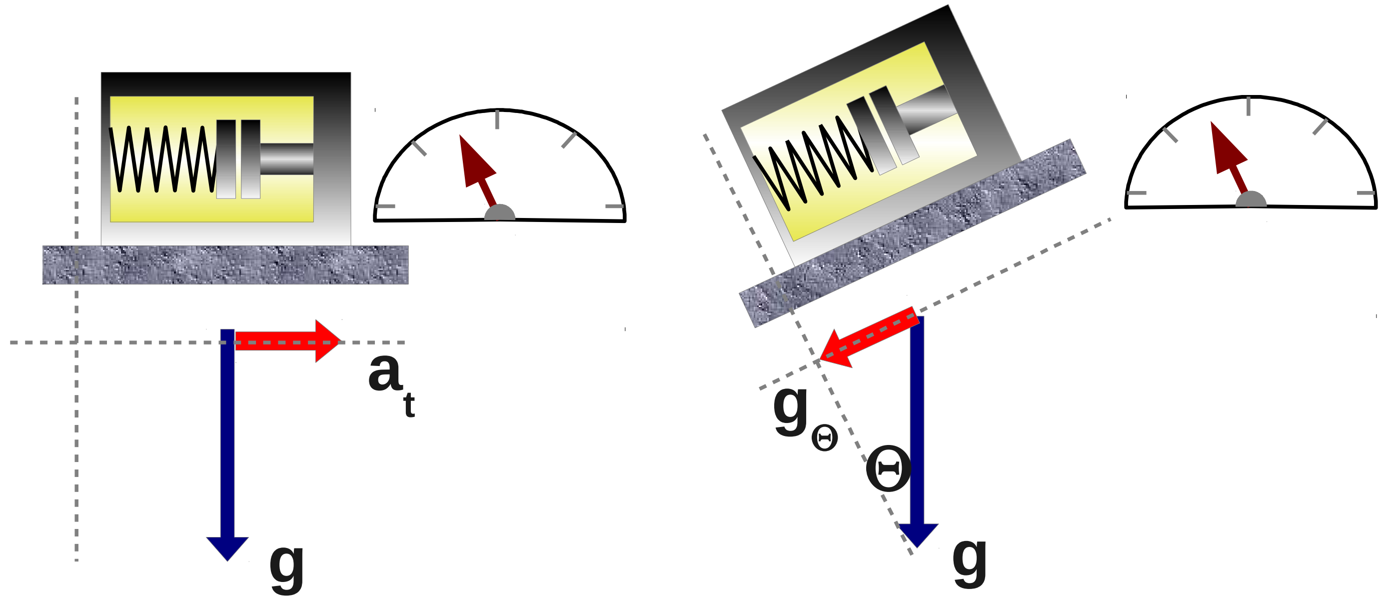

Dramatic consequences for the feedback!
(mainly during windy days)

Direct measurements of tilt are needed
(10^{-8} rad/sqrt(Hz) around 30 mHz)

- Extend the control to the 6 d.o.f.

-Improve the low frequency sensitivity of the GW antenna.

Optical detection of rotation

Sagnac Interferometers

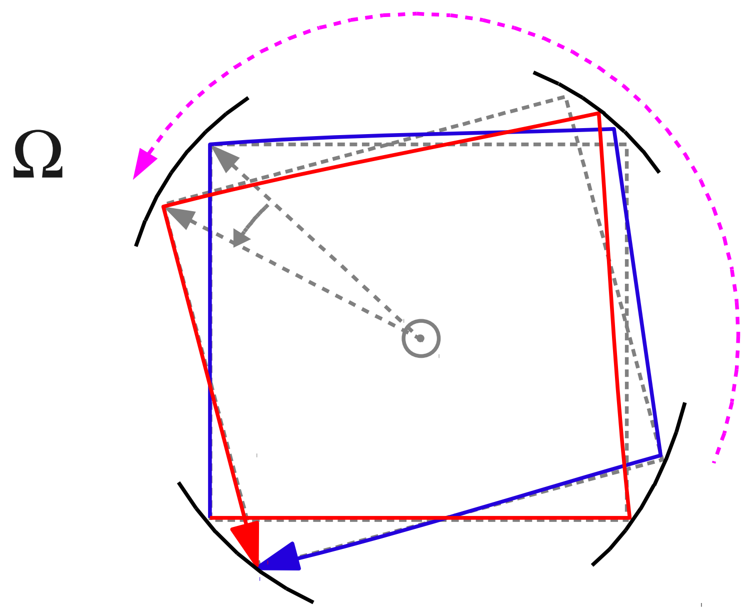

$$\Delta f_{Sagnac} = 4 \frac{A}{P\lambda} \vec{\Omega} \circ \vec{n}$$

- Absolute, scalar sensor
- No signal for a linearly accelerating reference-frame (No movable masses)
- No need of arrange arrays (single station measurement --> high resolution)

1.4 m GeoSensor

2009 R&D study of "G-Pisa"

Geosensor design+perimeter cntrl.

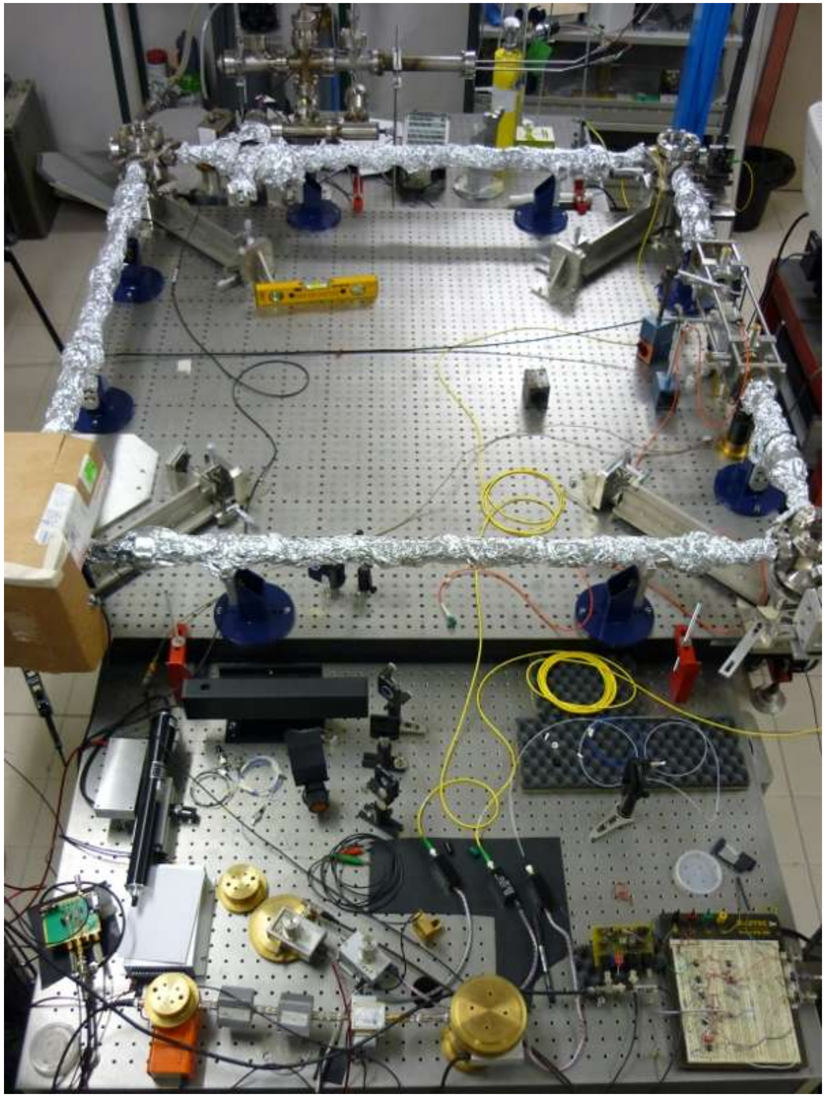

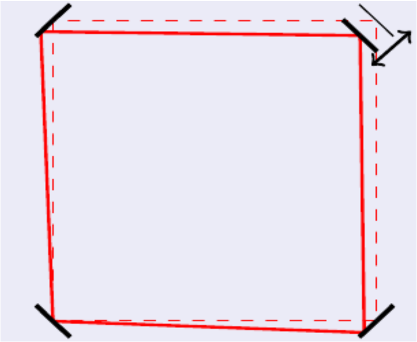

Perimeter stabilization using a movable mirror

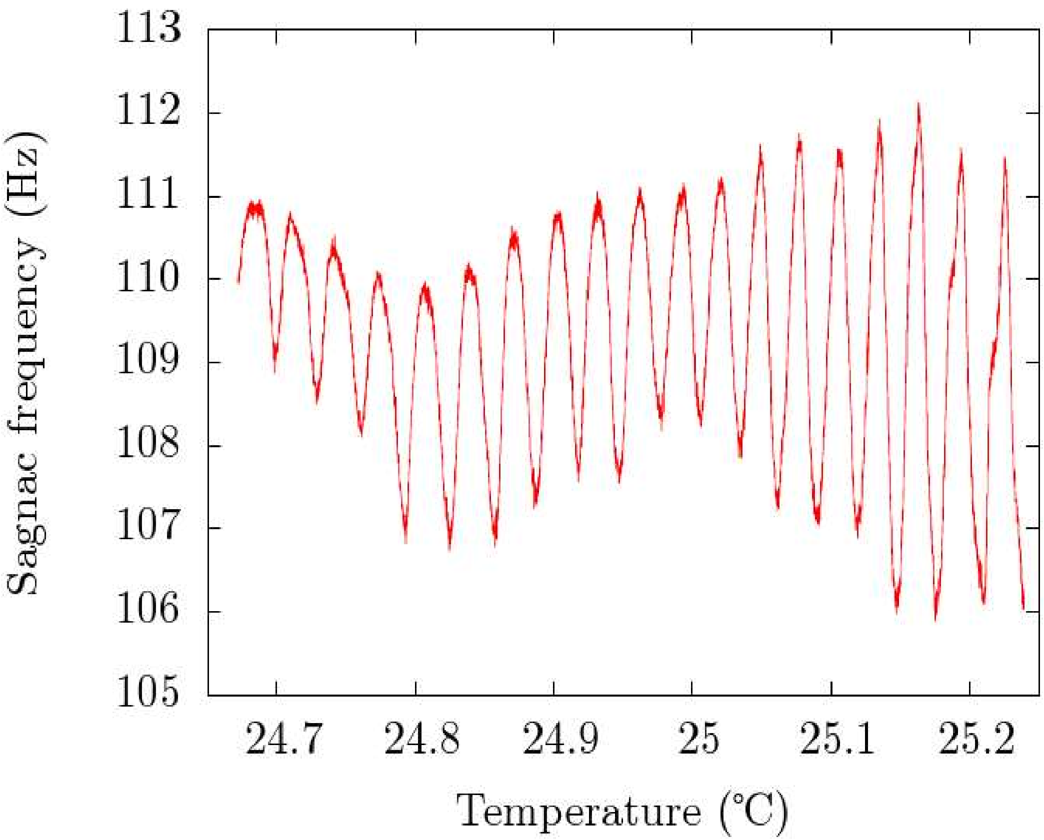

Backscattering phases (simulation)

Single actuator

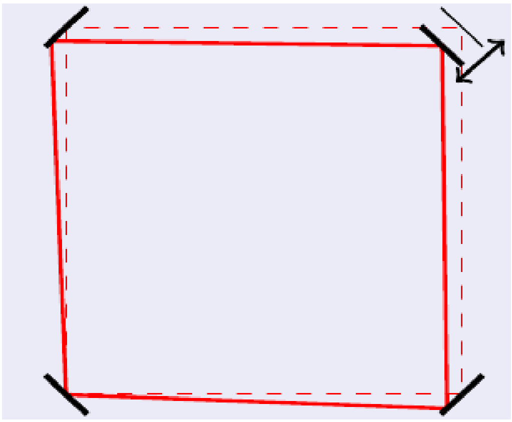

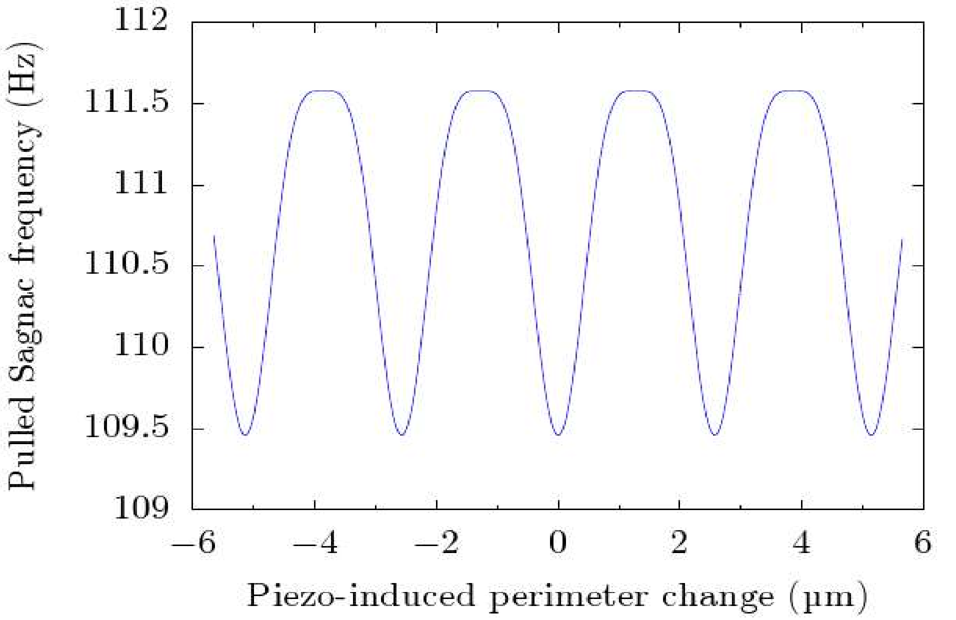

Better control of backscattering → More Symmetry!

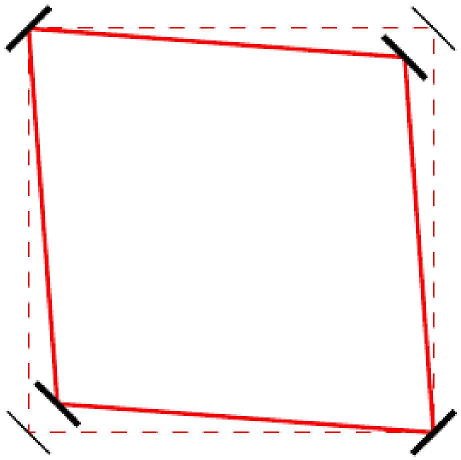

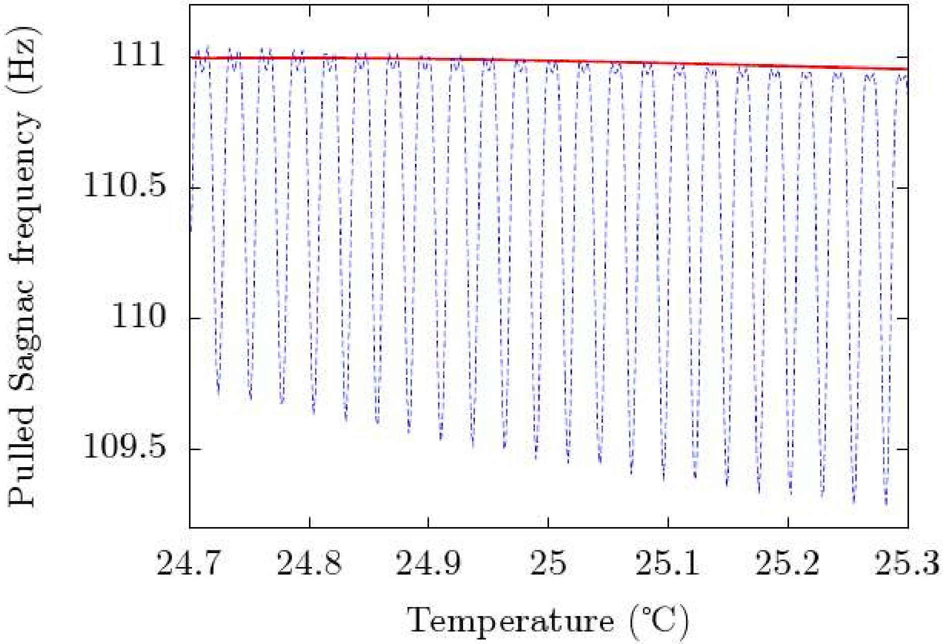

More symmetric scheme (experiment)

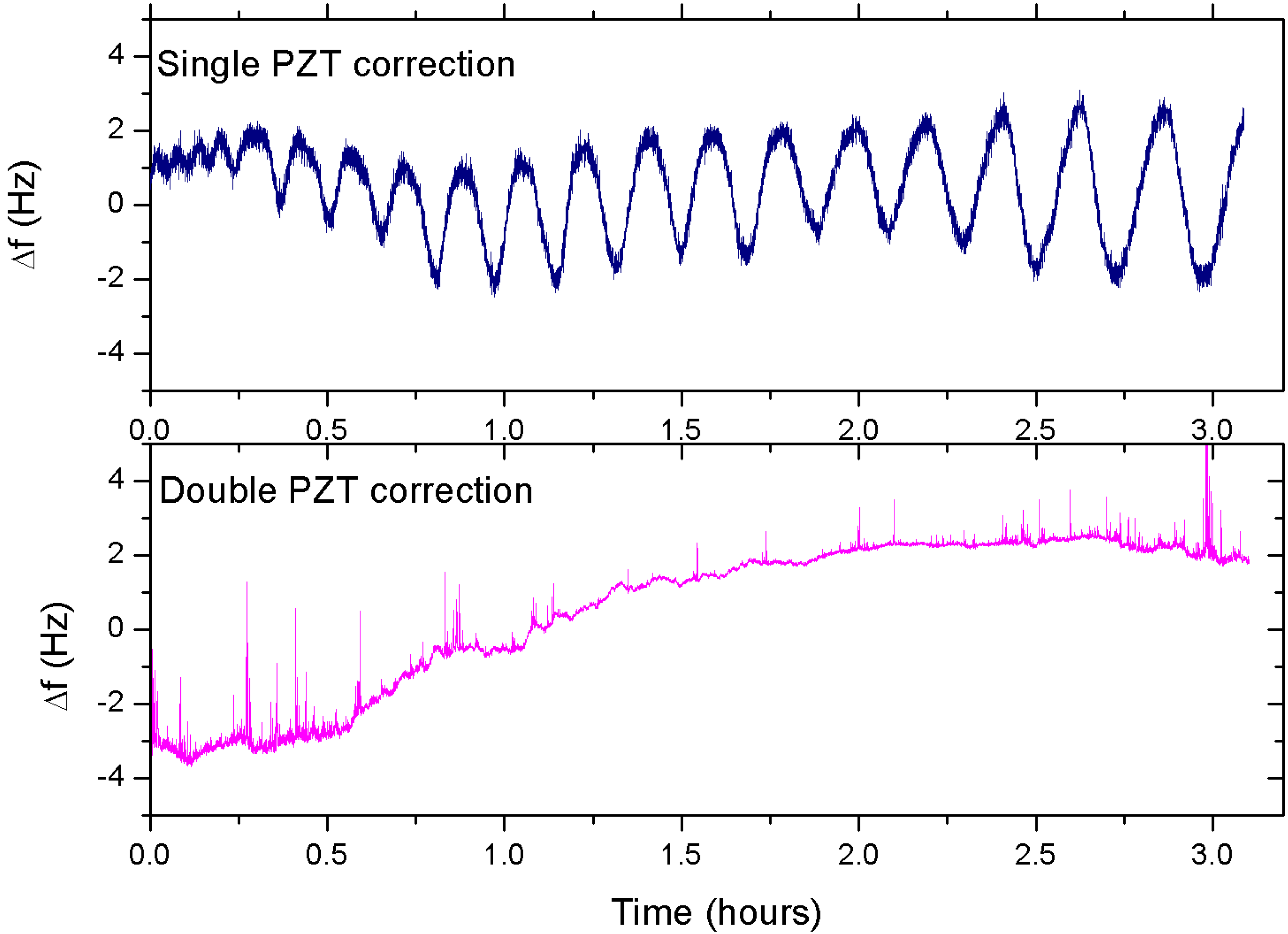

Installation in VIRGO

2010 Test run

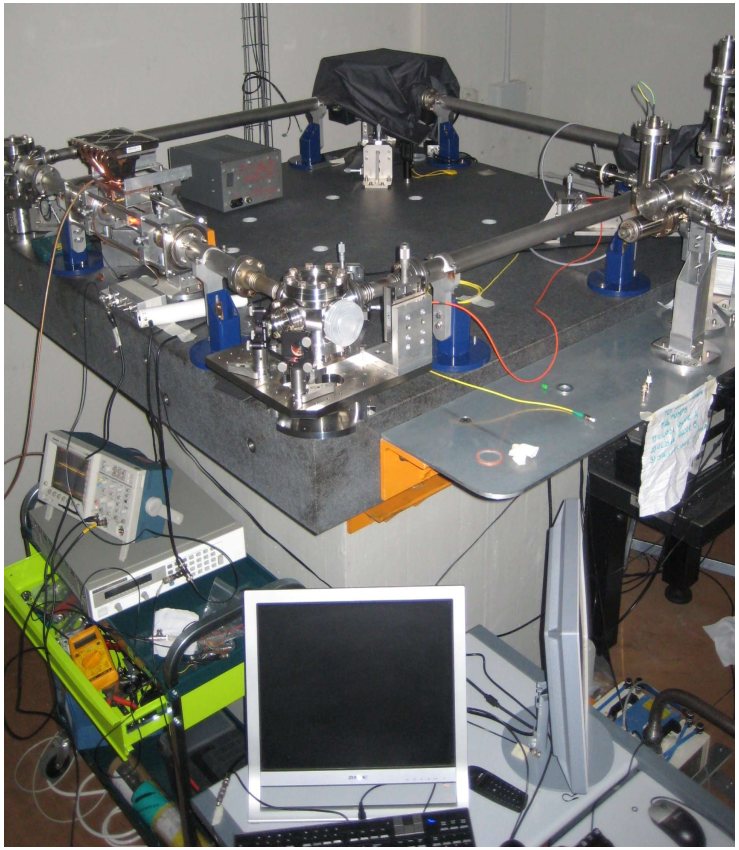

2011 Tilt meter configuration

Operation @ Virgo

Earth's Rotation (+ local rotations + systematics)

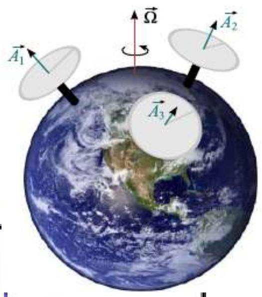

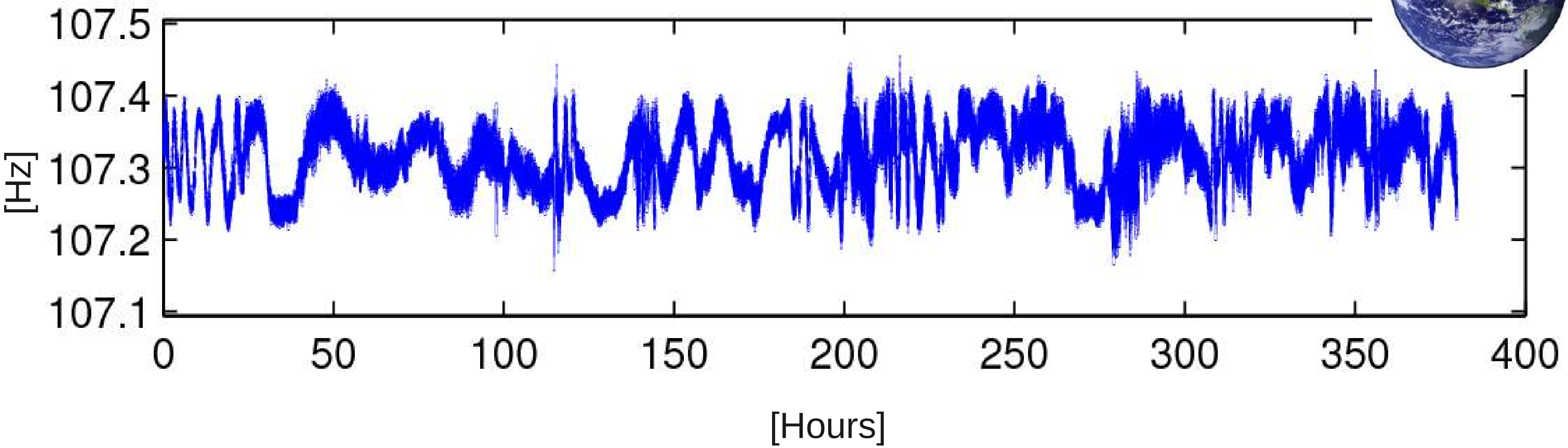

Angular Sensitivity Limit

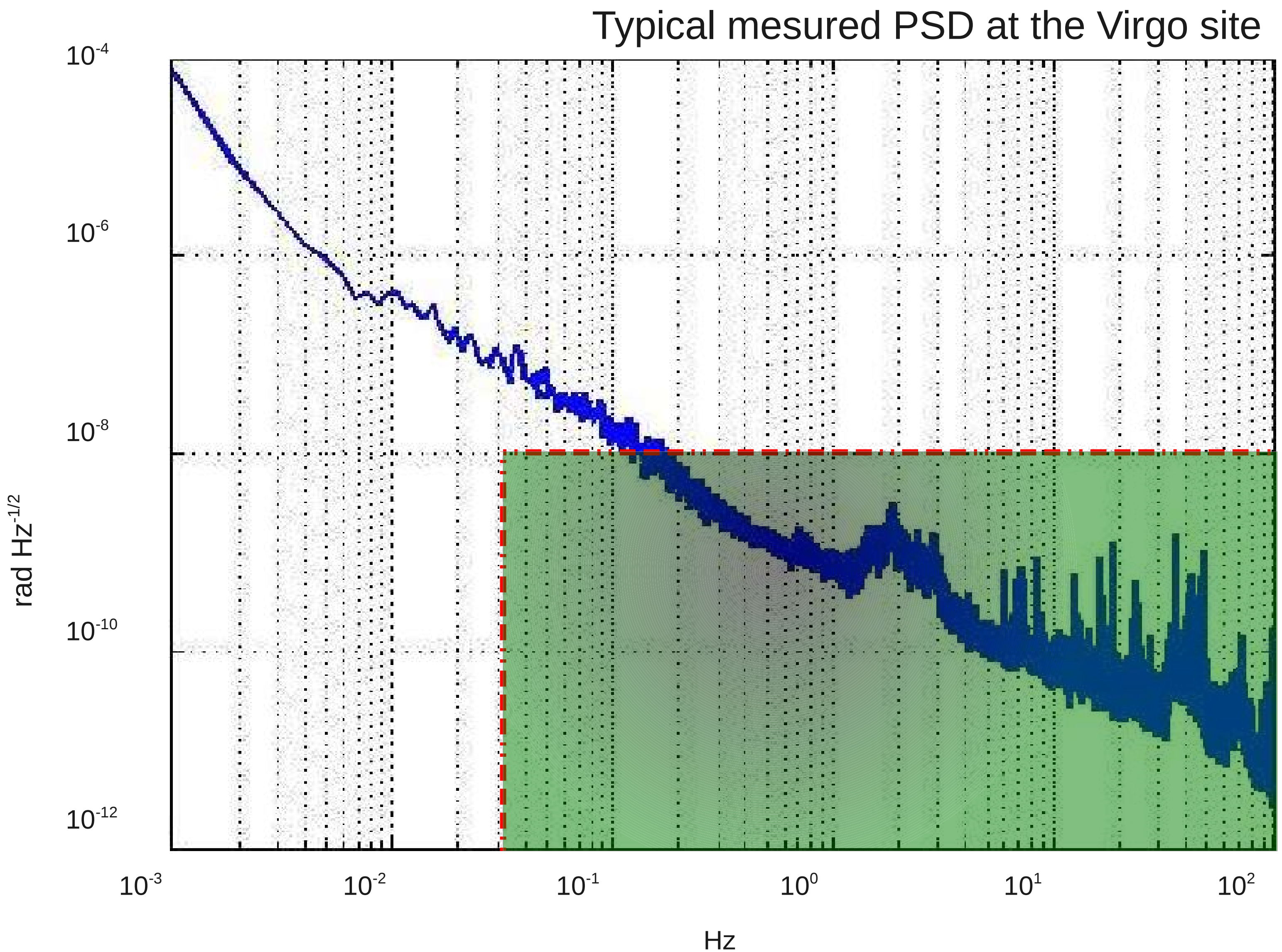

Environmental Monitoring

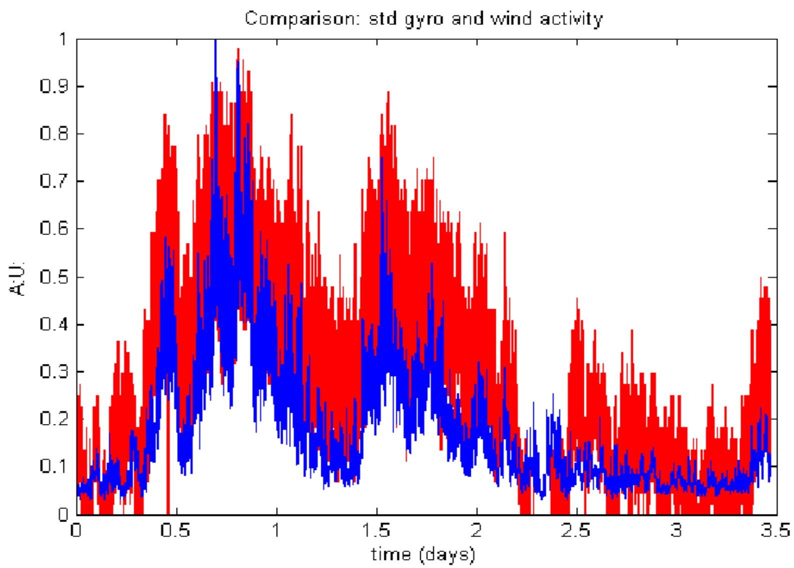

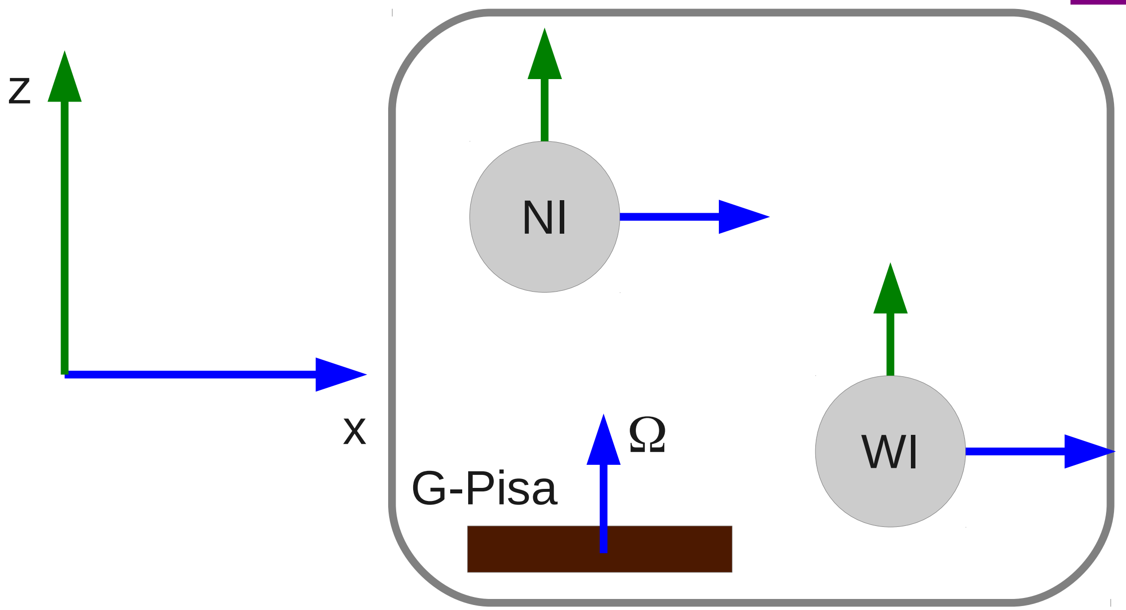

<u>"Cohere" analysis</u>

-Time length= 2 hours
-Window=2^8 s (Hamming)
-Overlap=50%

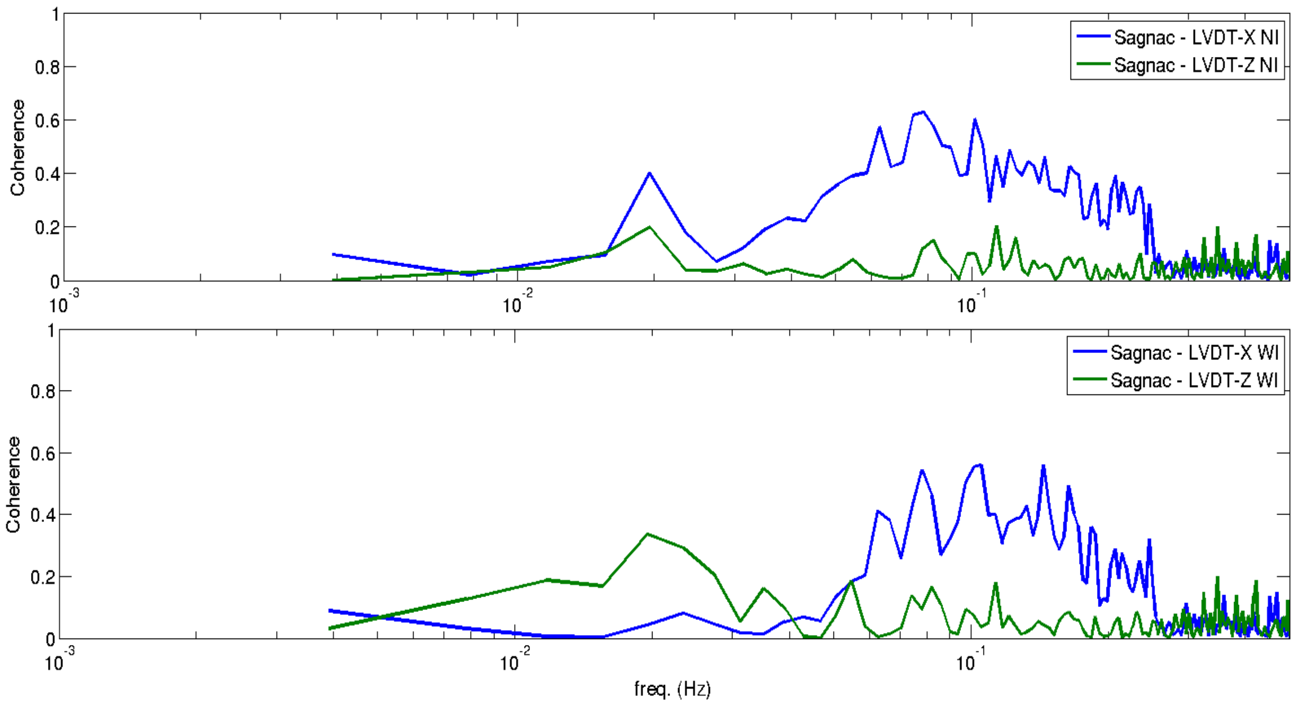

M_w=9.0, March 2011, Japan earthquake

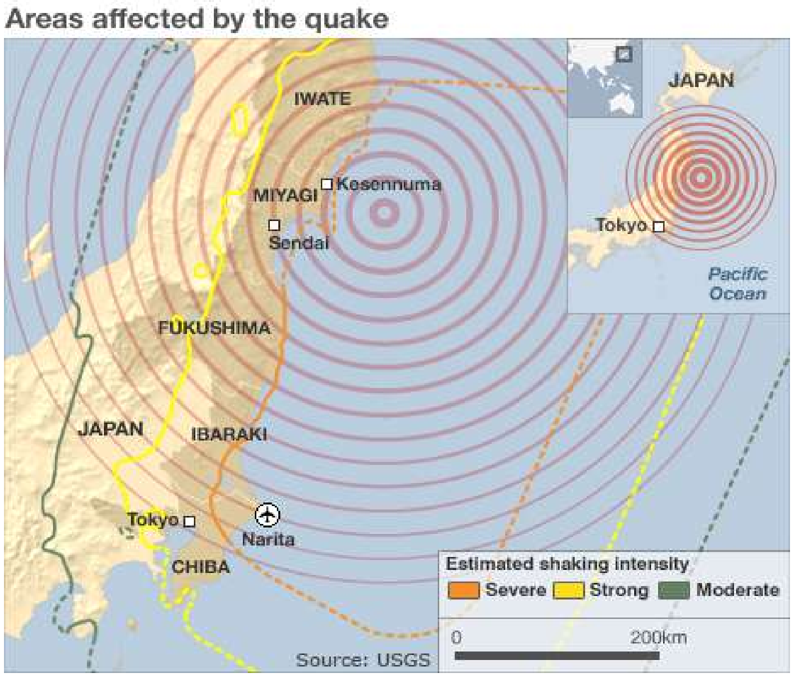

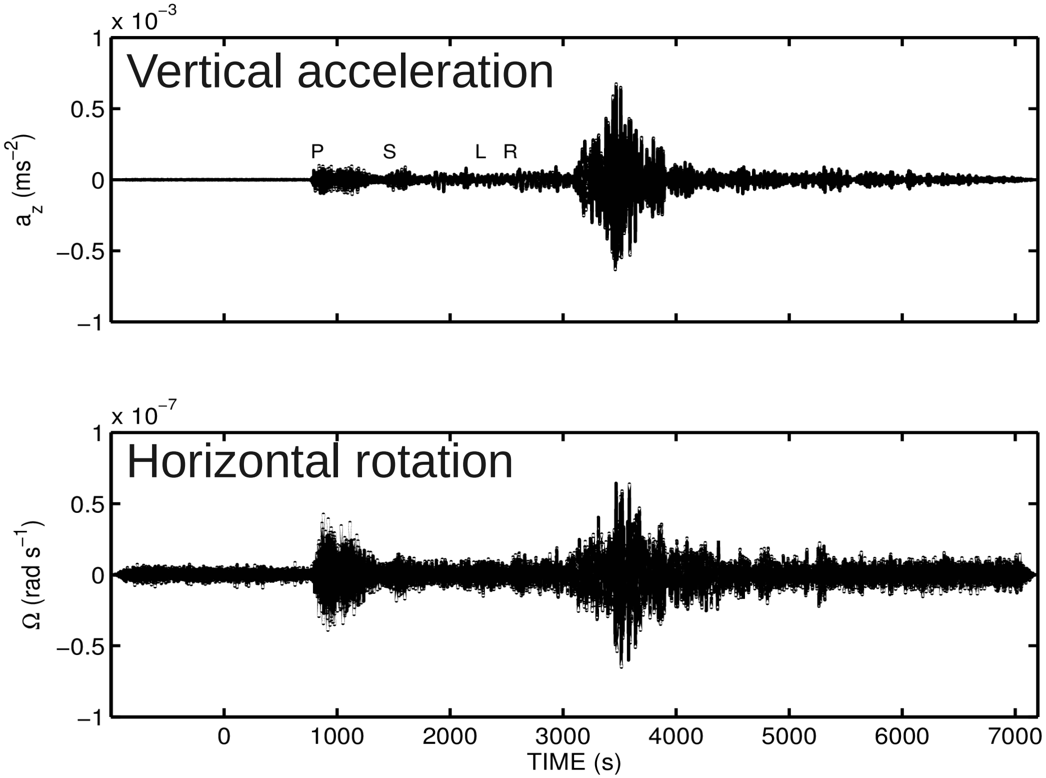

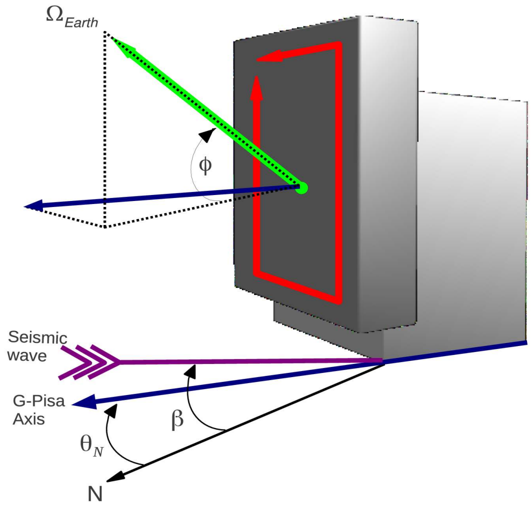

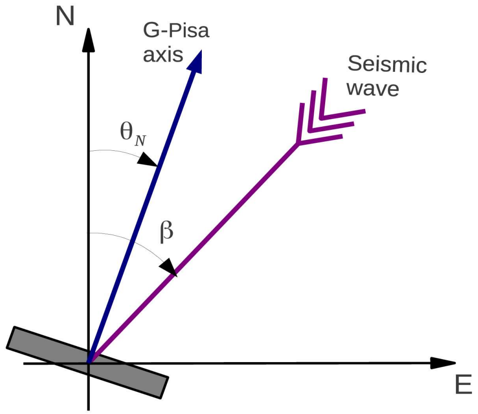

Horizontal Rotations detection scheme in Cascina (Pisa)

Rayleigh Analysis

Linear vertical acceleration (*Episensor*)

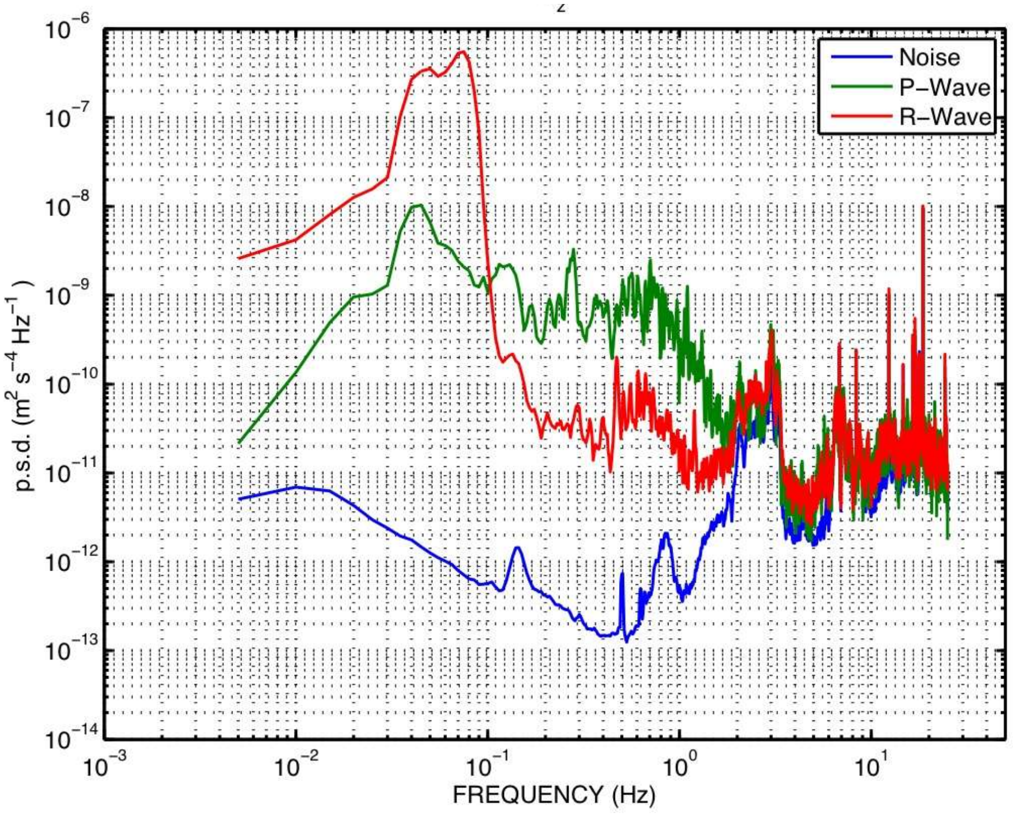

Rotation rate (*gyro*)

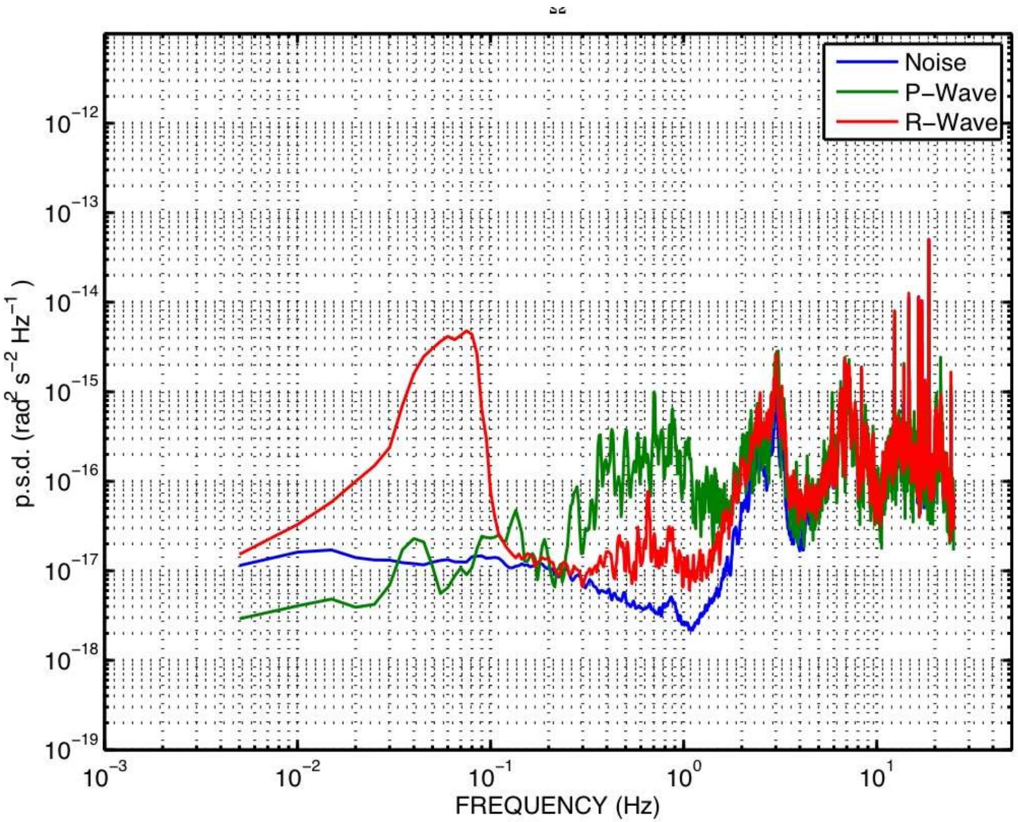

M_w=9.0, March 2011, Japan earthquake

1 hour around Rayleigh arrival; fl=0.9 × 1/T Hz; fh=1.1 × 1/T Hz,

$\left(a_z;\Omega_x\right)$

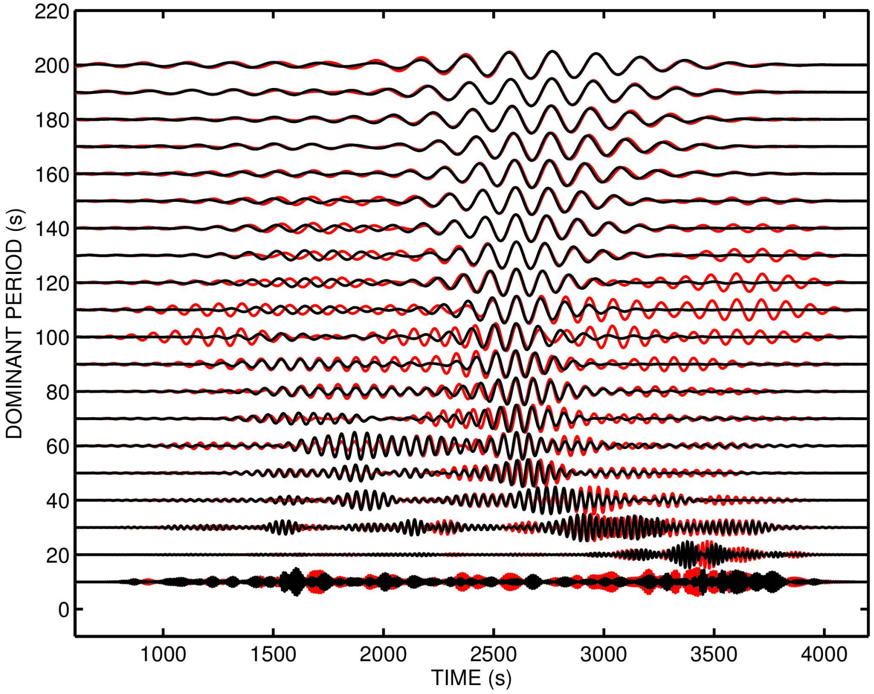

$Corr\left(a_z,\Omega_x\right)$

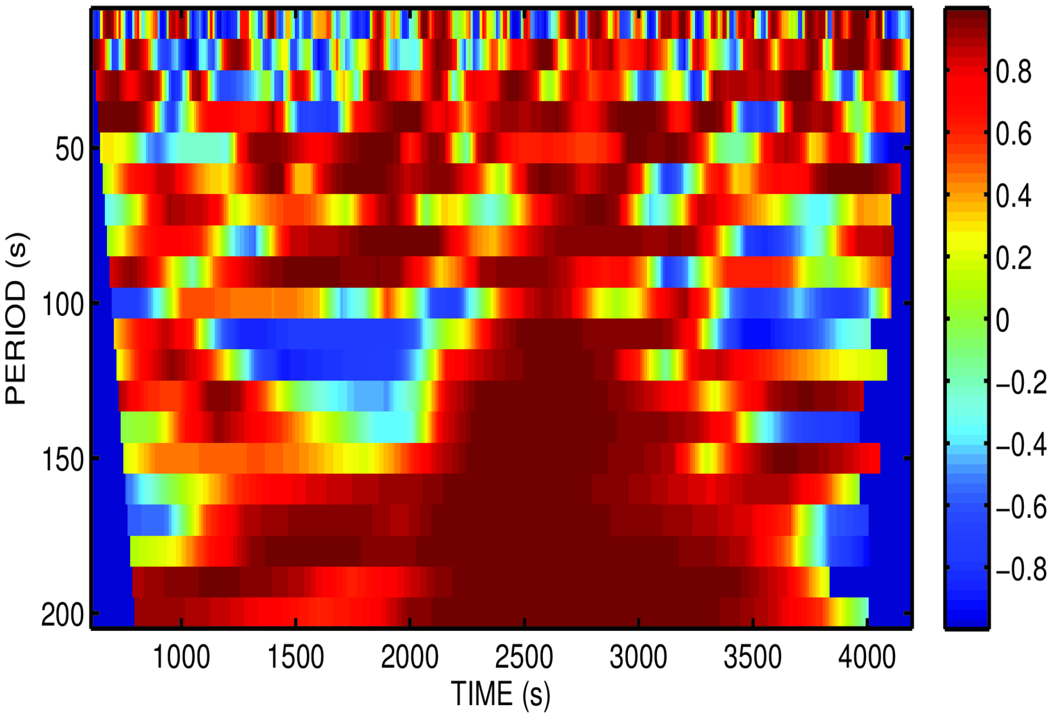

Seismic array analysis

Tri-axial accelerometers

Horizontal Rotations comparison

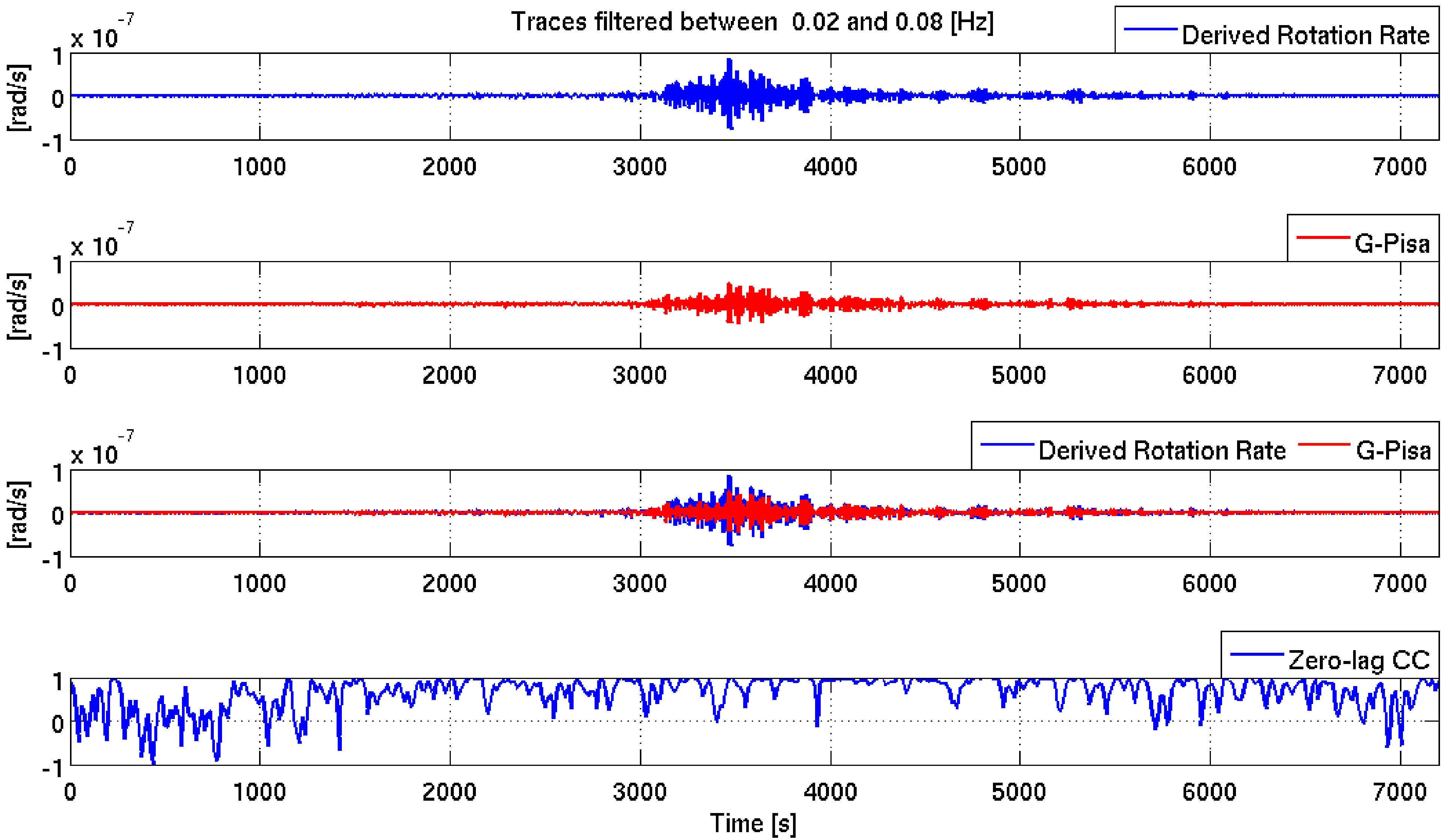

Seismic array analysis

Data from the array provide:

the surface waves velocity (**v**) and azimuth (ψ)

- ψ is used to correct Gyrolaser signal
- **v** is used to investigate dispersion properties

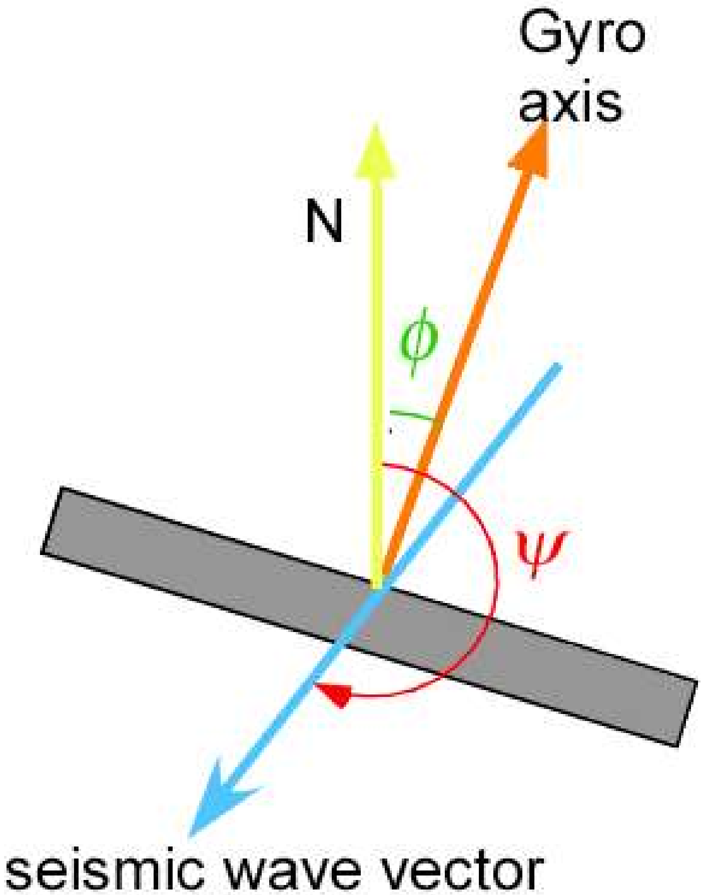

$$\Omega_T = \Omega_x \sin(\psi - \phi)$$

$$c_R = \frac{\ddot{u}_z}{\Omega_T} \qquad \ddot{u}_z = c_R \Omega_T$$

Rayleigh phase velocities

3 methods

Only array (multifrequency PWF)
Spectral ratio of collecated Rot. and acc.
Linear regression between collocated Rot. and acc.

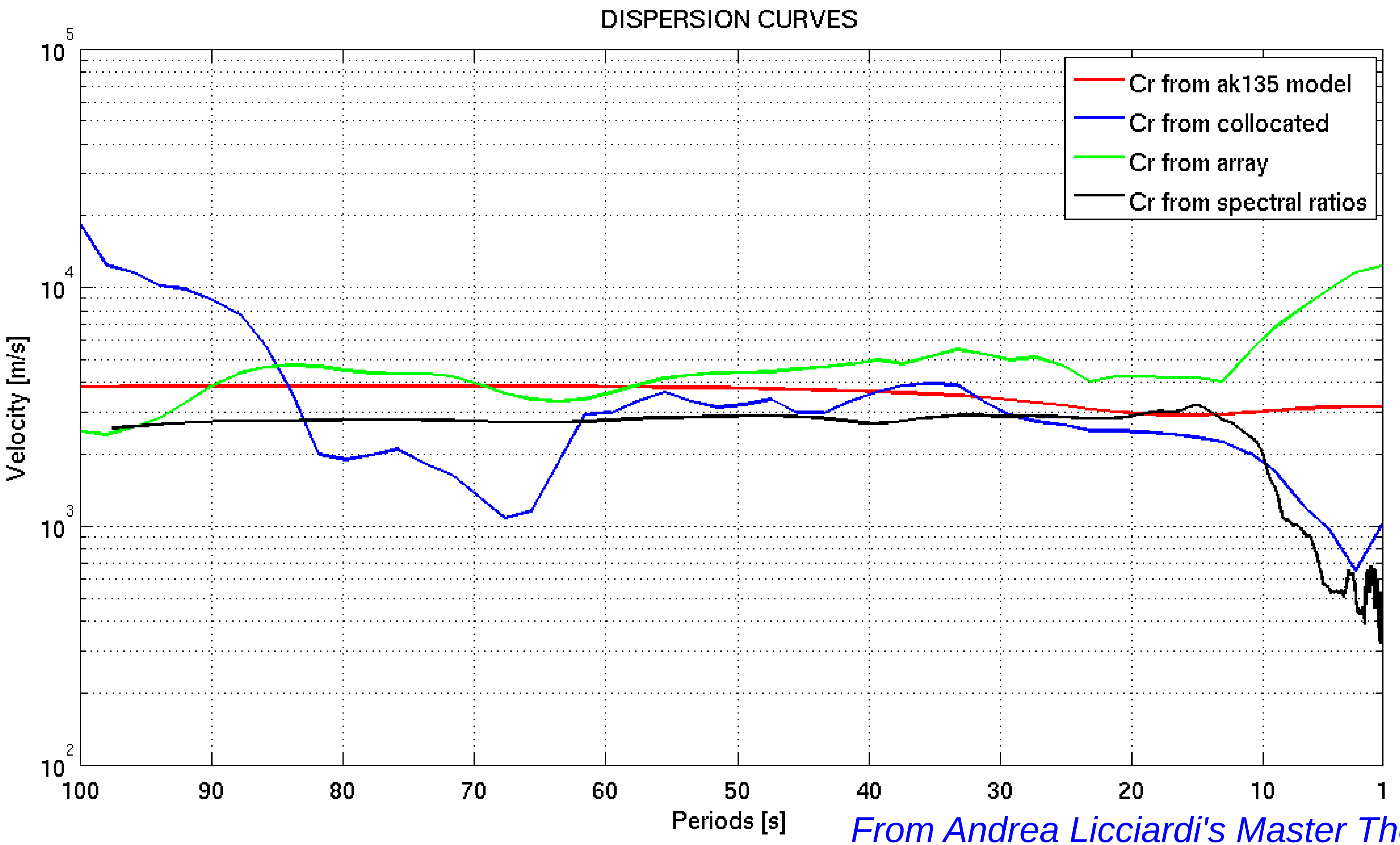

From Andrea Licciardi's Master Thesis.

Higher frequencies analysis

0.5-5Hz: highest sensitivity of the gyroscope

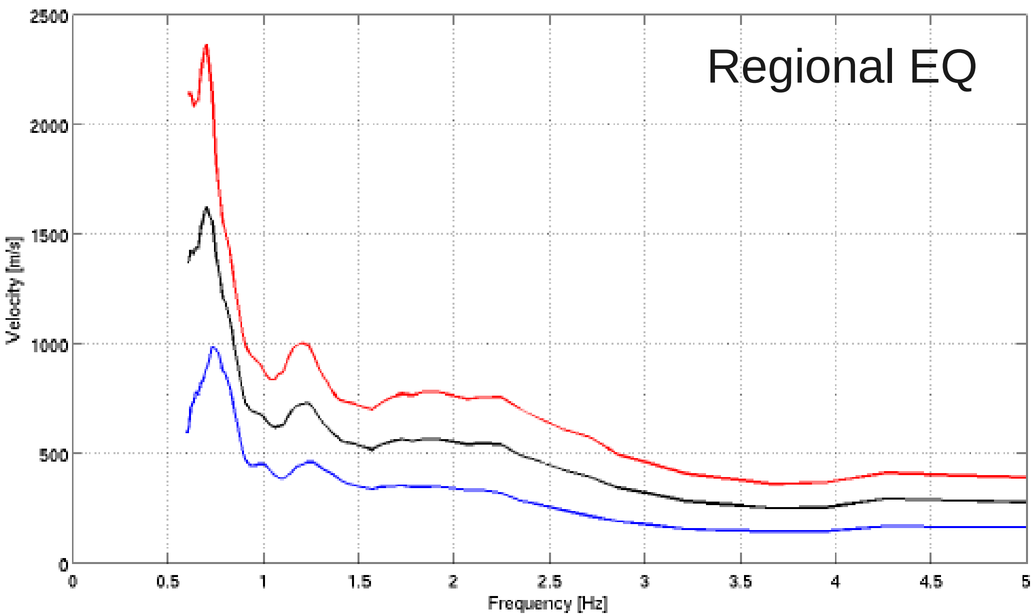

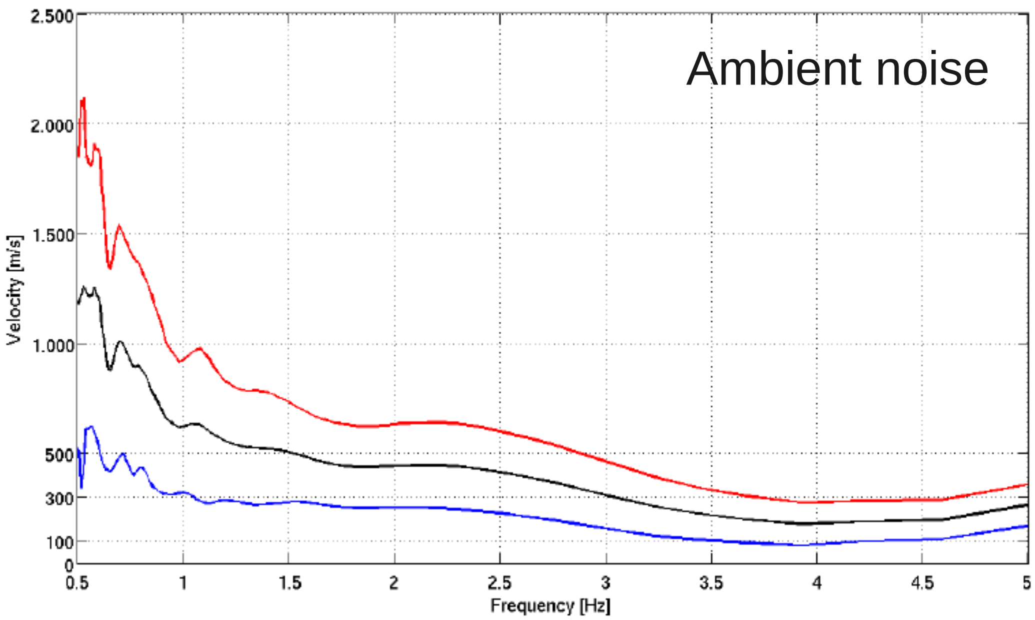

Rayleigh-waves dispersion curve for the MW = 4.9, July 17th,2011, earthquake. Velocities are obtained through a **linear regression between vertical acceleration** and rotation rate. ZLCC > 0.75.

Rayleigh-waves dispersion curve from collocated measurements of rotation and translation for a 5 hours long ambient seismic noise signal. **Linear regression** (ZLCC > 0.75).

Seismic noise in GranSasso Hall B

STS-2 on top of the granite table

April **2013** Underground Test

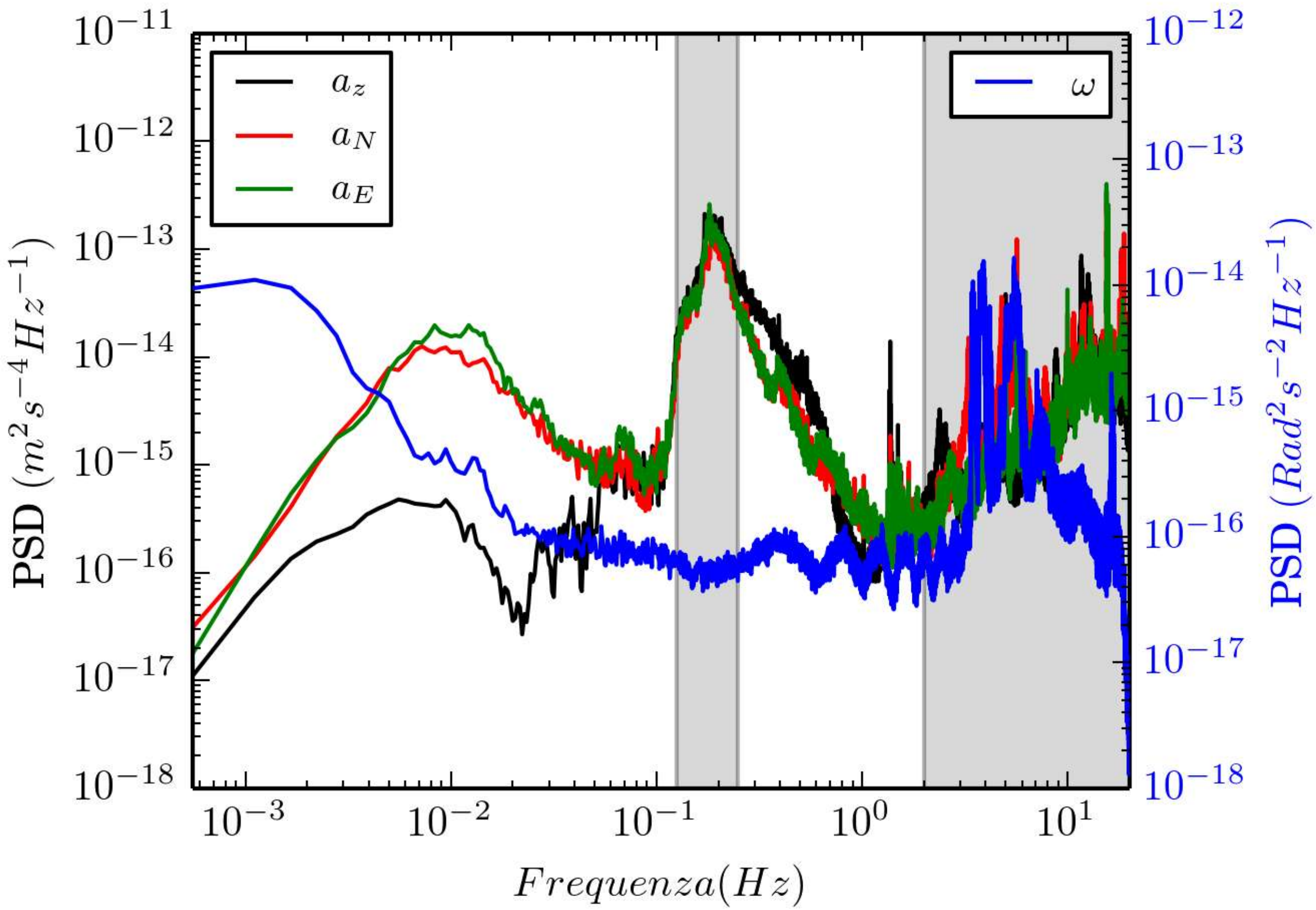

-Gyroscope **intrinsic noise**+l**ocal disturbances**:
no relevant correlations between translations and rotations (even during EQs!)

Larger RLG (L>3.5 m)+Dedicated isolation chamber

GINGER
(Giroscopes IN GEneral Relativity)

TESTING GR on Ground

Rotations in GENERAL relativity

*"The axis of a free-falling gyroscope precesses following the curvature of space-time due to **Earth's Mass** (Geodetic precession) and **Earth's Rotation** (Frame Dragging)"*

Present results: Earth orbiting Satellites

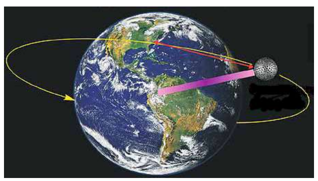

LAGEOS

Gravity Probe

LARES

A laser gyroscope located on GROUND:

$$\delta\vec{\Omega} \simeq \frac{G\,M}{c^2\,R}\Omega_E \sin\theta\,\hat{e}_\theta + \frac{G}{c^2\,R^3} J_E\,\Omega_E\left[\hat{j}_E - 3(\hat{j}_E\cdot\hat{u}_r)\,\hat{e}_r\right]$$

Geodetic: $6.98\,10^{-10}\,\Omega_E$

Lense Thirring: $2.31\cdot 10^{-10}\,\Omega_E$

- **COMPLEMENTARITY** to SPACE TESTS
- **NO NEED ANY EARTH MODELLING**
- **VECTOR** maesurement: relevance in **GEODESY** and **GEOPHYSICS**

Detection Strategy

F. Bosi et al., Phys. Rev. D 84, 122002 (2011)

Ground based rings

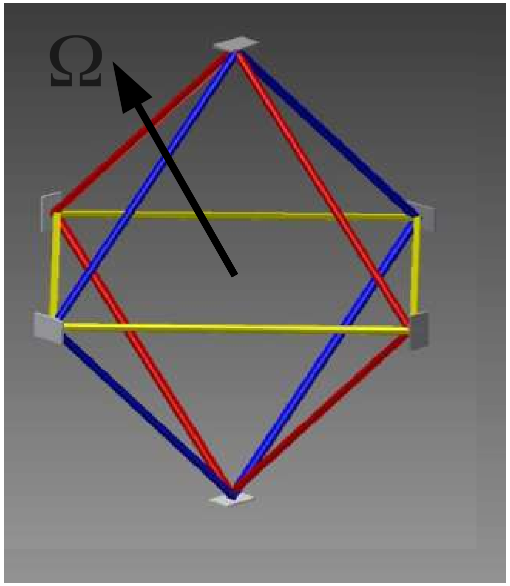

IERS 05C04

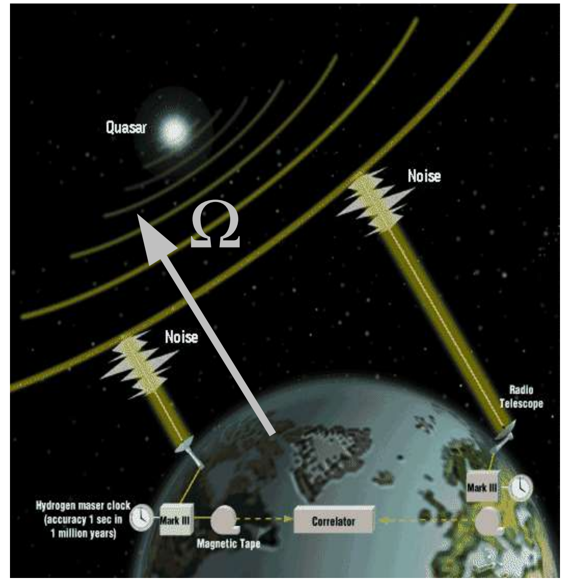

Compare the moduli (invariant)

$$\delta\Omega = \Omega_E^{local} - \Omega_E^{IERS}$$

$$\frac{|\delta\Omega|}{|\Omega_E|} \leqslant 10^{-10} \left(snr > 1 \right)$$

from:

$$\Delta f_i = \frac{4 A_i}{P_i \lambda_i} \vec{\Omega} \cdot \hat{n}_i + systematics$$

Sensitivity: Increase the scale factor (side-lenght > 6 m)

Geometry: lengths and relative orientations

Refer lengths to optical references (including diagonals Fabry-Perot)

OCTAHEDRON solves for relative angles (only lengths measurement)

Laser dynamics

Plasma and cavity effects must be modelled and controlled to the required accuracy.

Relative rotational noise

UNDERGROUND laboratory (Gransasso)

Toward GINGER: Geometry control

$$\Delta f_{Sagnac} = \boxed{4\frac{A}{P\lambda}}\vec{\Omega}\cdot\vec{n} + syst.$$

S

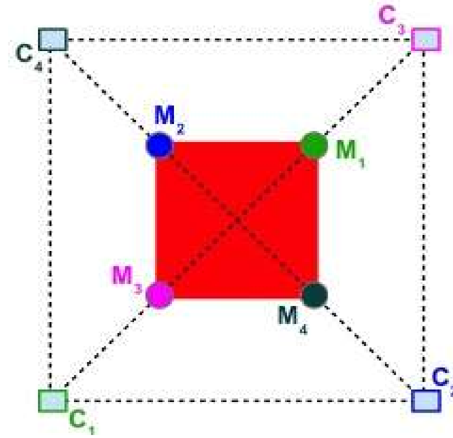

12 d.o.f.
-6 d.of. (Rigid body)
= 6 d.of. (Cavity deformation)

Scale-factor normal modes

"Kite" mode 2 d.o.f.

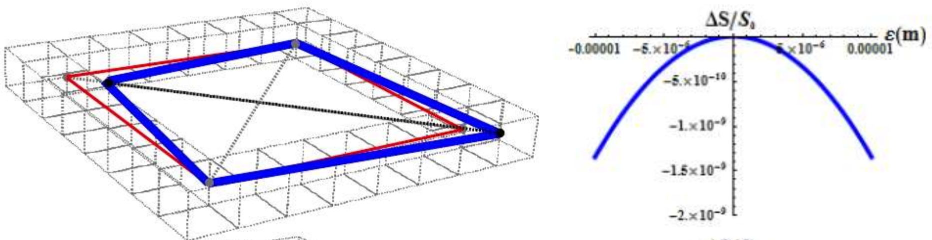

"Out of plane" 1 d.o.f.

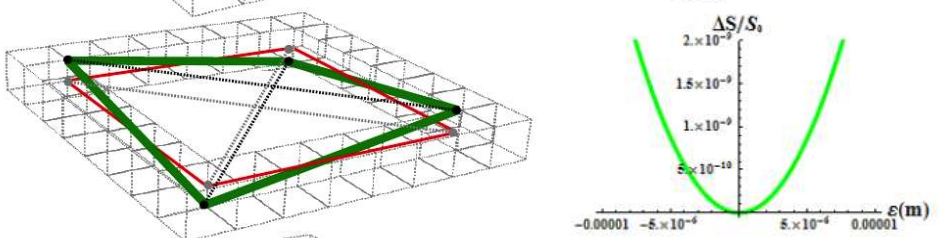

Relative rotation 1 d.o.f.

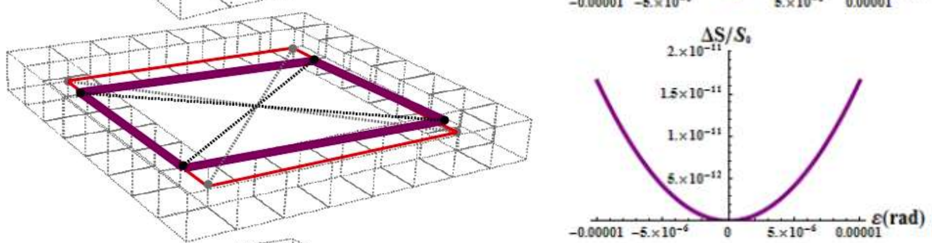

"Streching" 2 d.o.f.

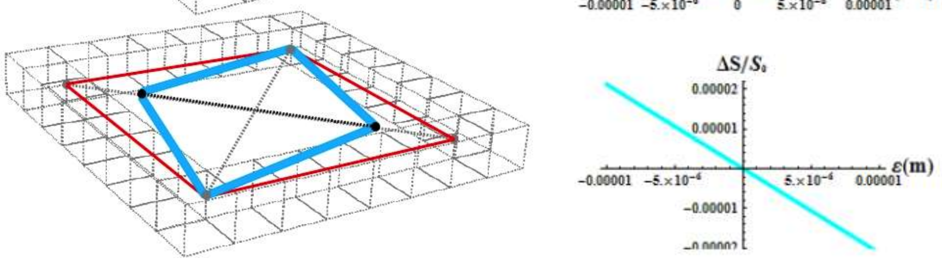

Experimental technique

3 observables: perimeter length+2 diagonals length (absolute)

Strategy: optimize the perimeter by moving the four mirrors along the normal modes directions

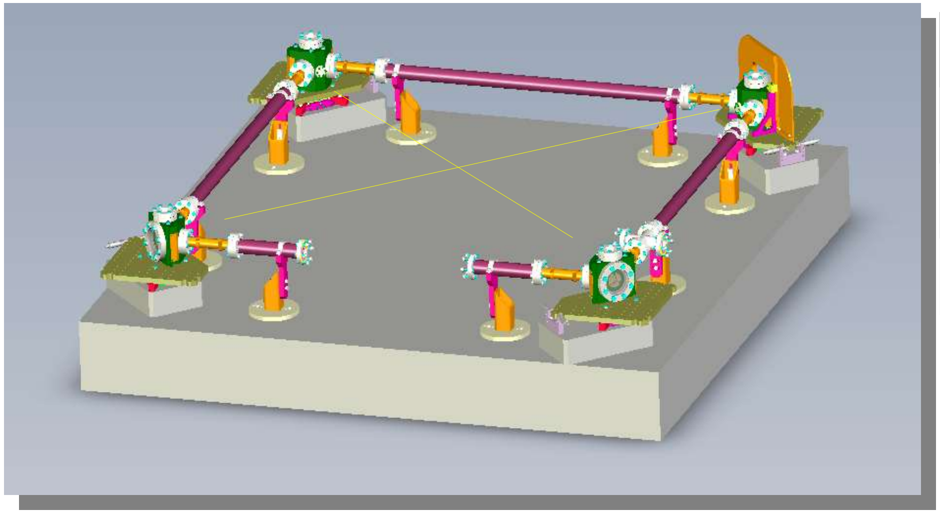

GP-2 RingLaser
Side 1.60 m
6 PZT: 1 3D+3 1D
Open access to diagonals

Reference of length:
I_2-He-Ne frequency standard

Perimeter control
Measure beat frequencies:
Gyro/Iodine + two gyro modes

Diagonals control
Use a diode laser (locked to the Iodine)
Inject the Fabry Perot cavities
Measure FSR + Absolute wavelength

Interrogation System: First tests

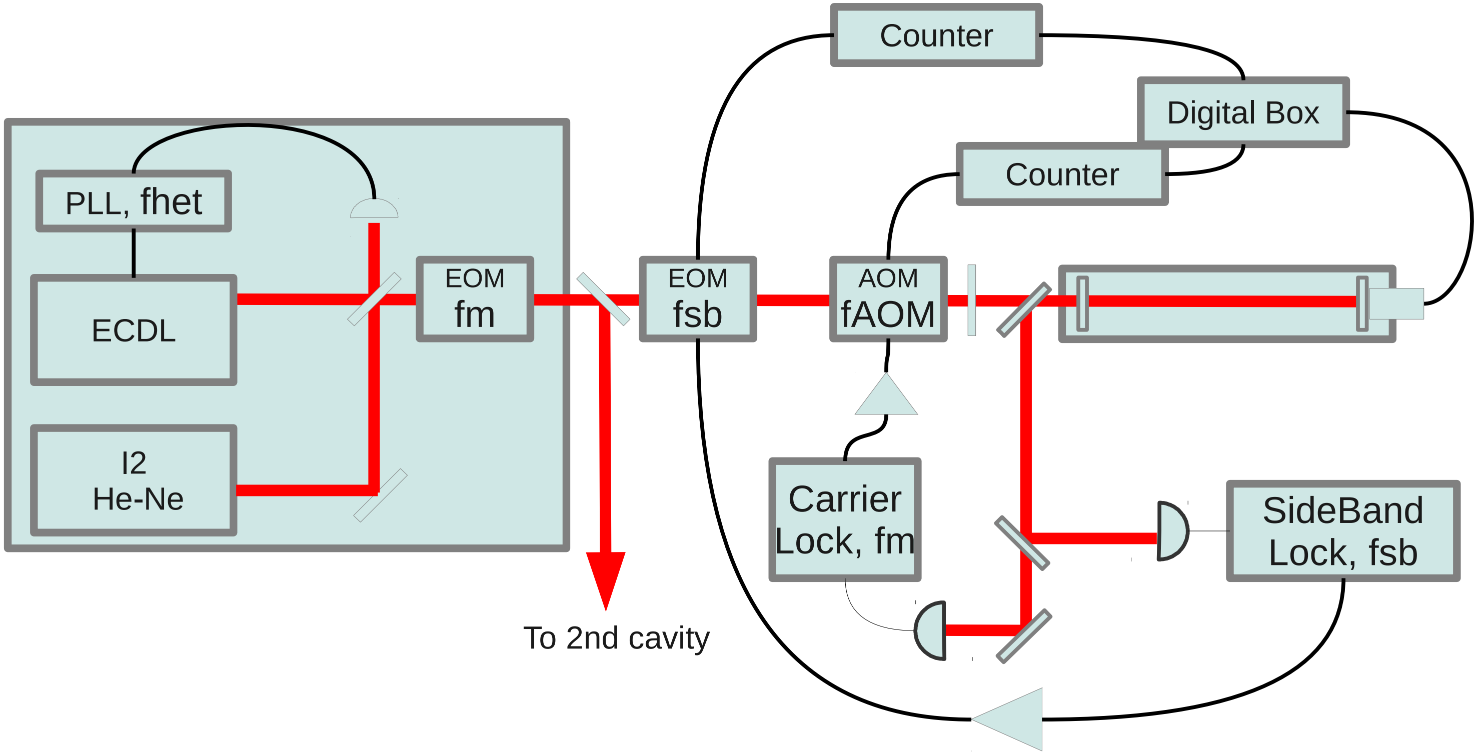

Carrier Lock

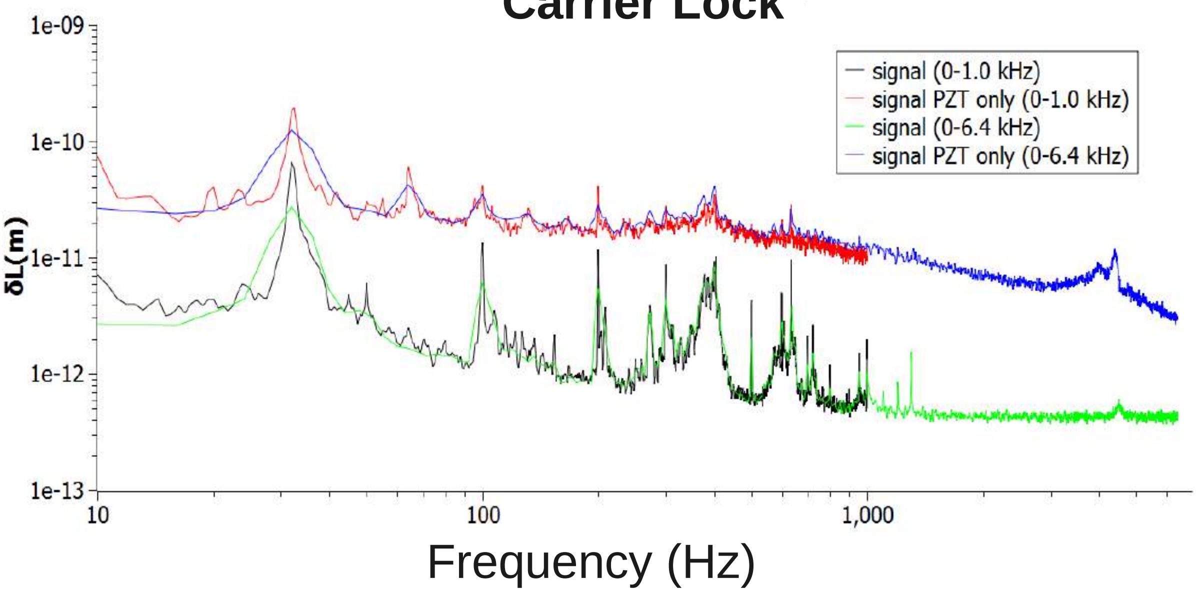

2 FSR Sideband error signal

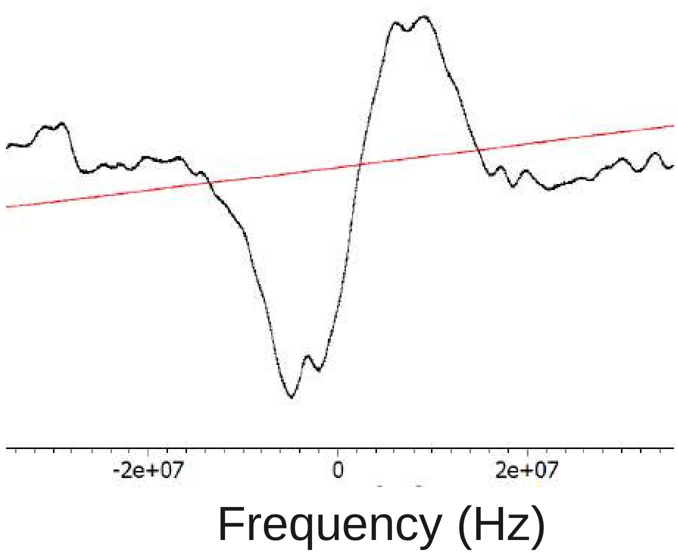

Ring laser "hacking"

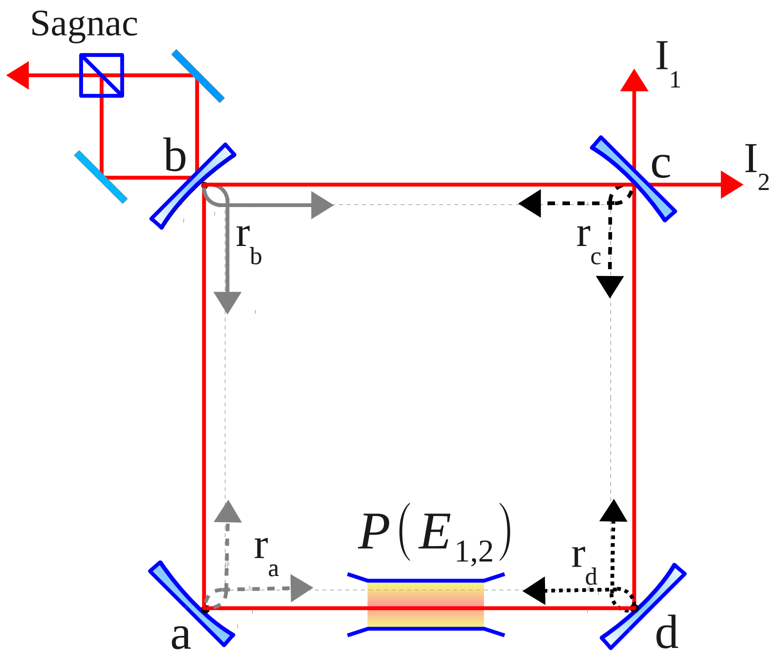

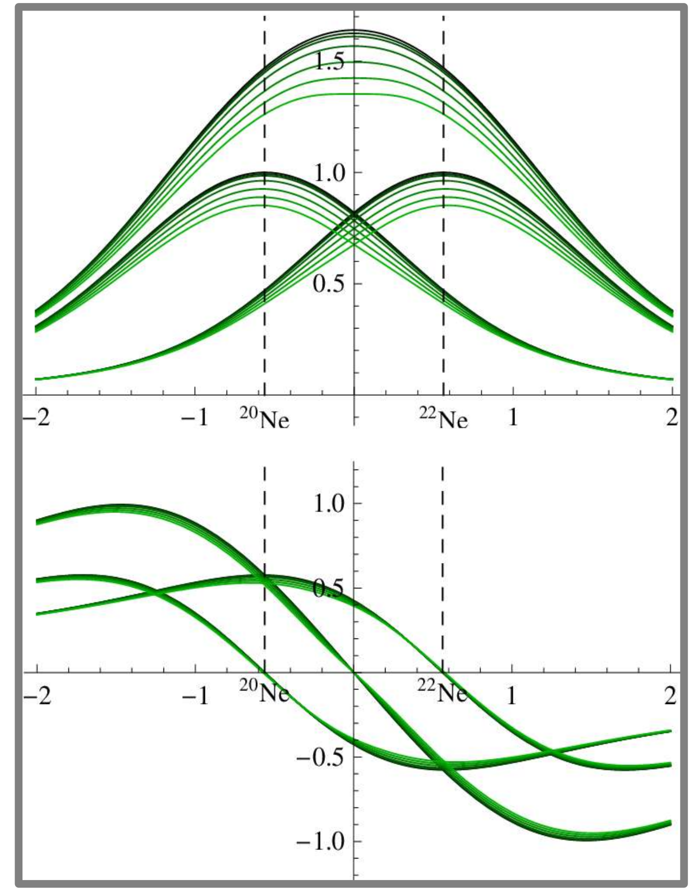

Active medium He+²⁰Ne+²²Ne

$$P^{(3)}(E_{1,2}) = \frac{-2i\mu_{ab}^2}{\gamma_{ab}} \int_{-\infty}^{\infty} \chi_{1,2}(v)\,\rho^{(2)}(v, E_{1,2})\,dv$$

Opposite beams dynamics

$$\dot{I}_1 = \alpha_1 I_1 - \beta I_1^2 - \theta_2 I_2 I_1 + r_2\sqrt{I_1 I_2}\cos(\psi - \epsilon_2)\ ,$$
$$\dot{I}_2 = \alpha_2 I_2 - \beta I_2^2 - \theta_1 I_2 I_1 + r_1\sqrt{I_1 I_2}\cos(\psi + \epsilon_2)\ ,$$
$$\dot{\psi} = \omega_s + \tau_1 I_1 - \tau_2 I_2 - r_2\sqrt{\frac{I_2}{I_1}}\sin(\psi - \epsilon_2) - r_1\sqrt{\frac{I_1}{I_2}}\sin(\psi + \epsilon_1)$$

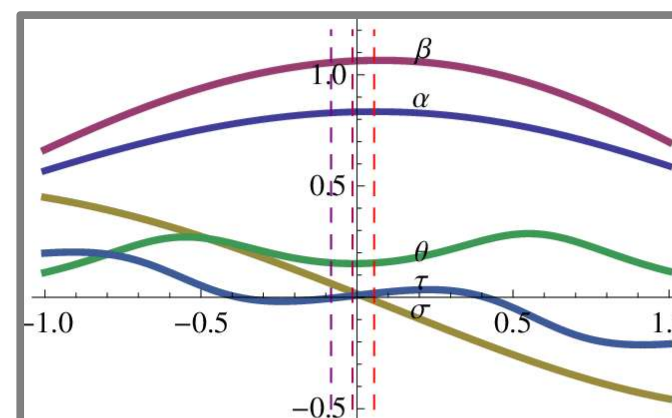

Kalman filter principle

1. Identification: start from perturbative solutions in $r_{1,2}$

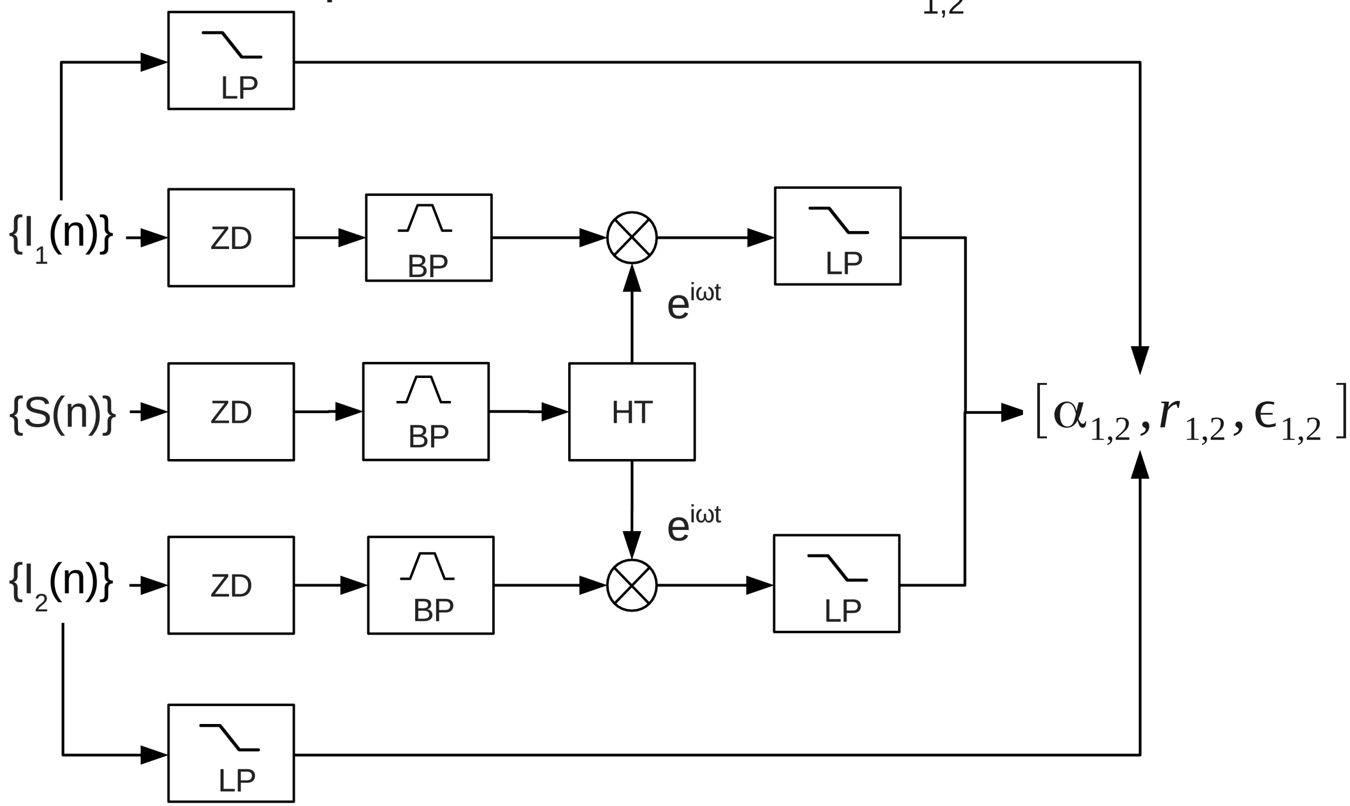

2. Filtering:

$$\left|\dot{\psi}-\omega_s+\tau_1 I_1-\tau_2 I_2-r_2\sqrt{\frac{I_2}{I_1}}\sin(\psi-\epsilon_2)-r_1\sqrt{\frac{I_1}{I_2}}\sin(\psi+\epsilon_1)\right| \Rightarrow \omega_s$$

*Beghi et al., Applied Optics **51**, 31 (2012)*

The **accuracy** strongly depends on the knowledge of the **gain medium** !

Gain calibration method

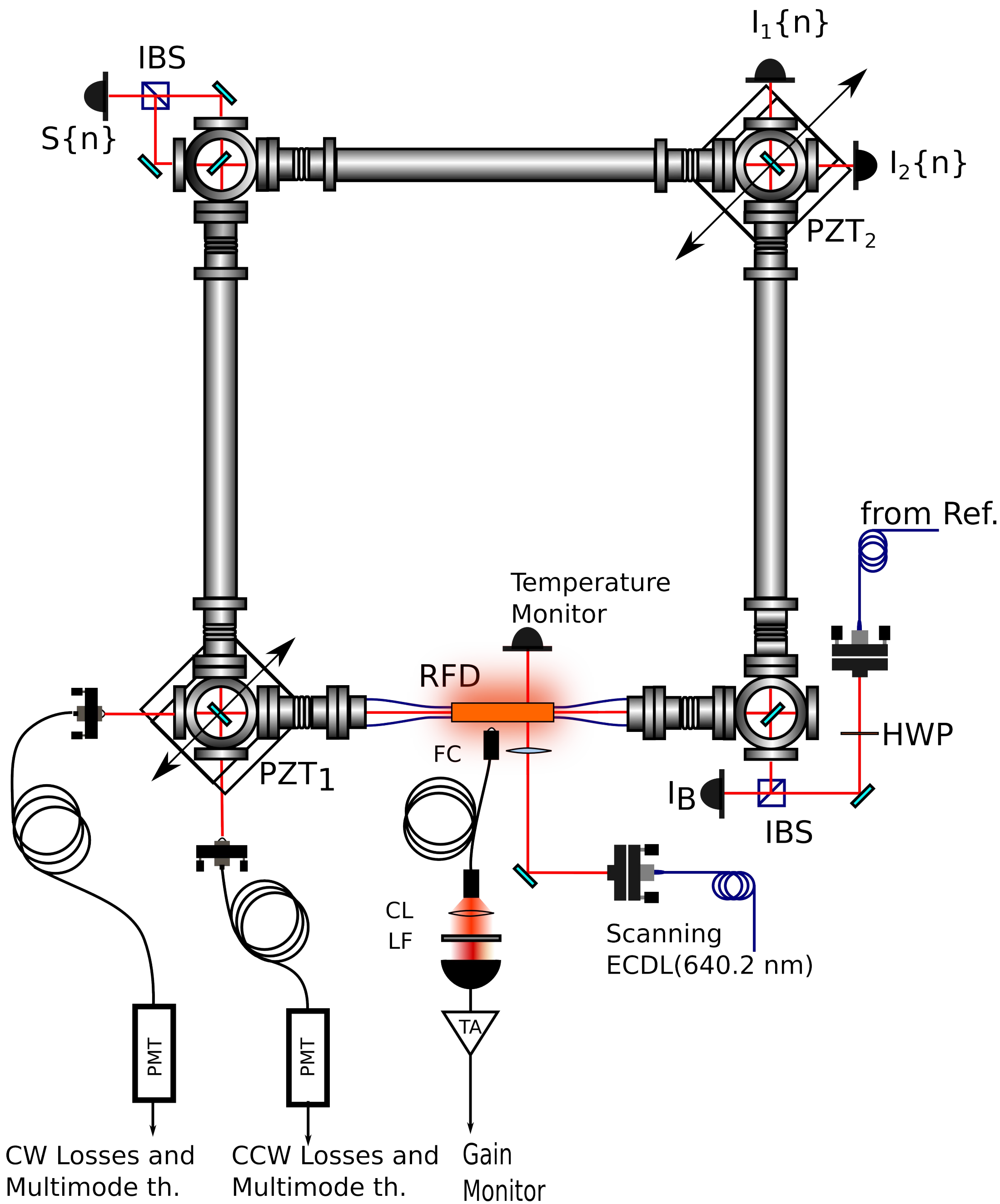

1. Set the optical detuning.
Lock the perimeter at the maximum gain

2.Calibrate gain-losses monitor.
Ramp RF power recording the fluorescence monitor

3.Determine losses (RDT)

4.Measure plasma temperature and composition
Absorption spectroscopy at 640.2 nm

5. Set the system scale at the multimode transition
Looking at the second mode birth.

The experiment

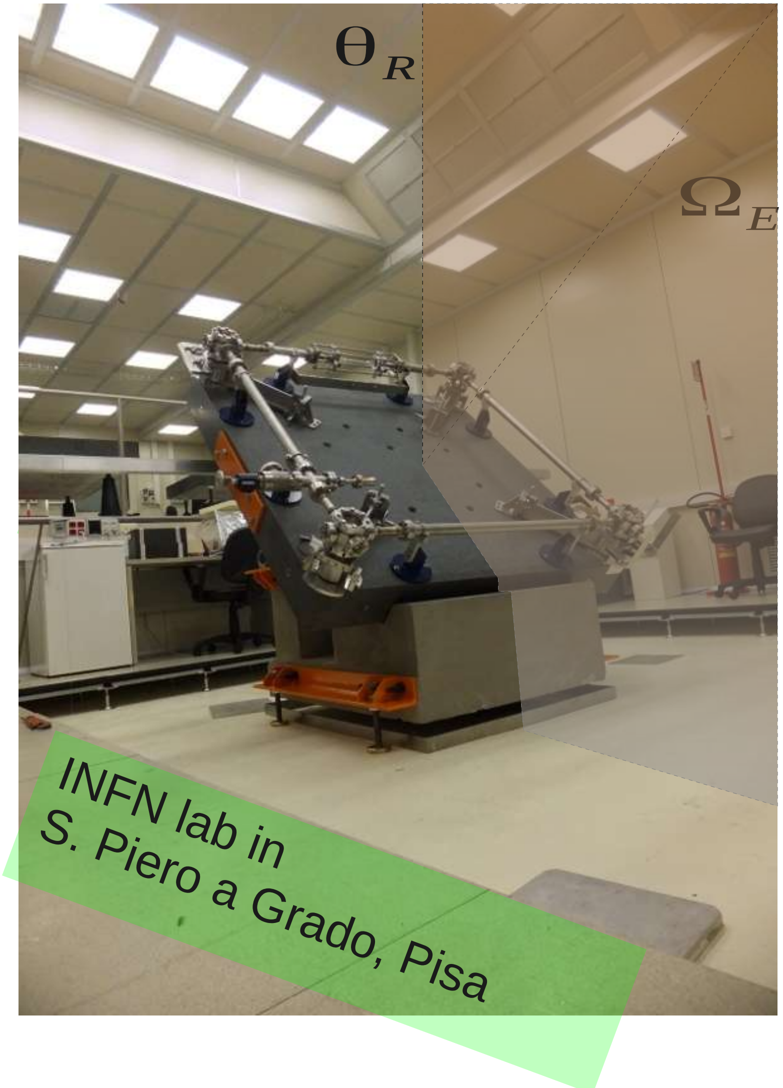

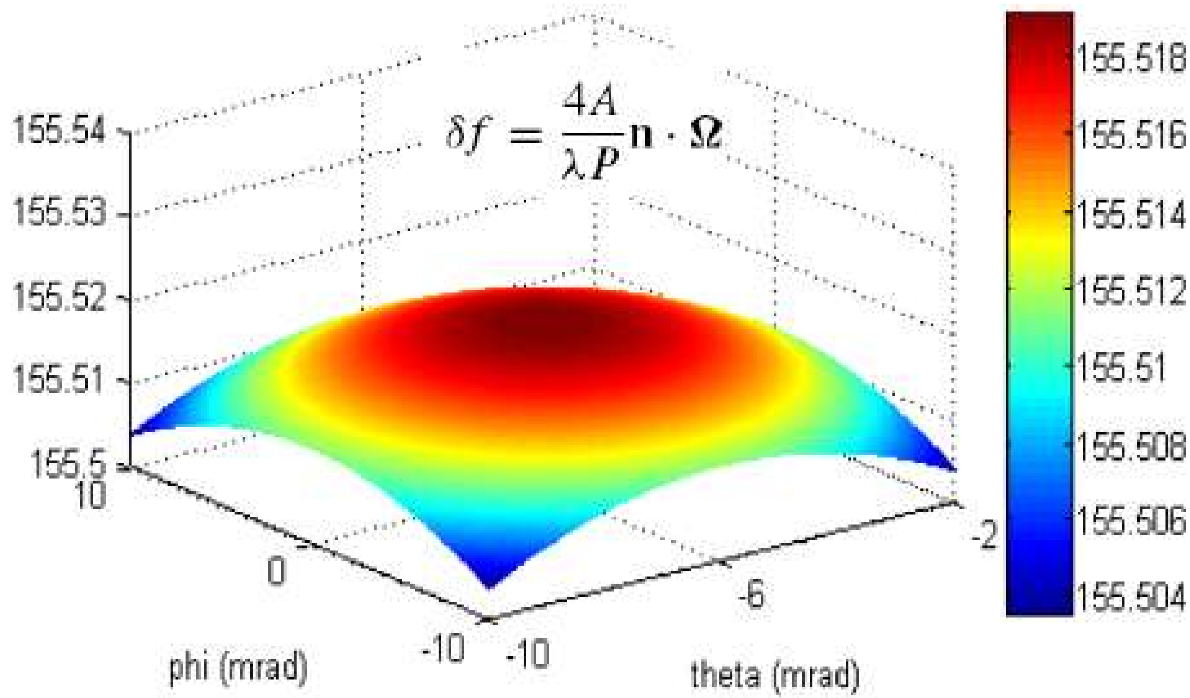

-Maximum Sagnac frequency

-Minimum contribution from orientation error

-Reduction of the effect of local tilts

-Larger distance from the lock-in threshold

Good for addressing systematics and accuracy...

Direct observations of laser parameters

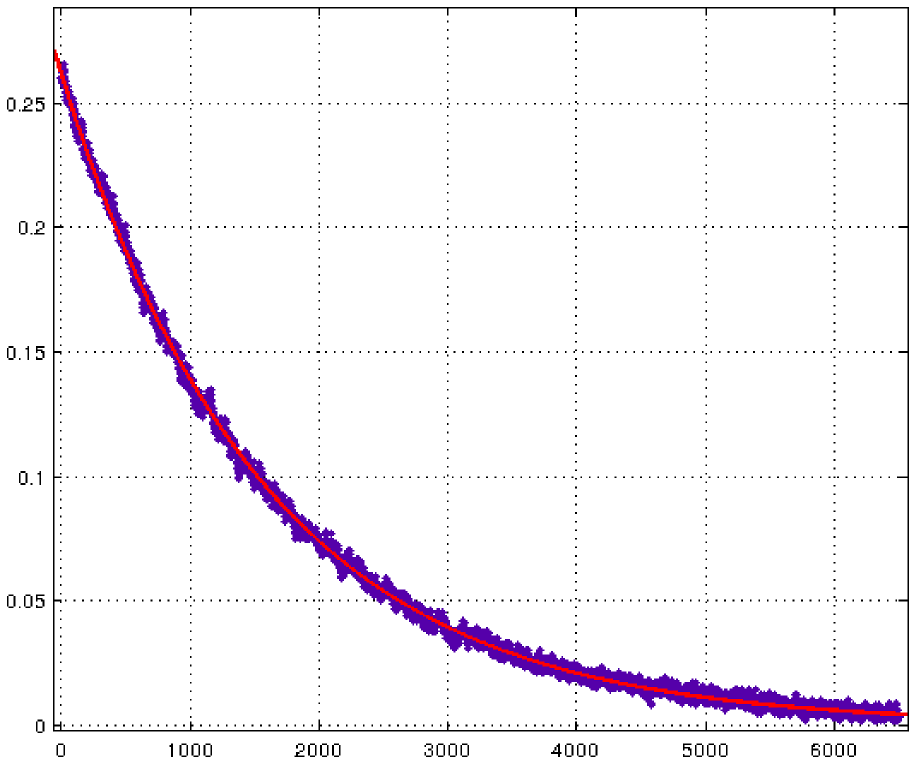

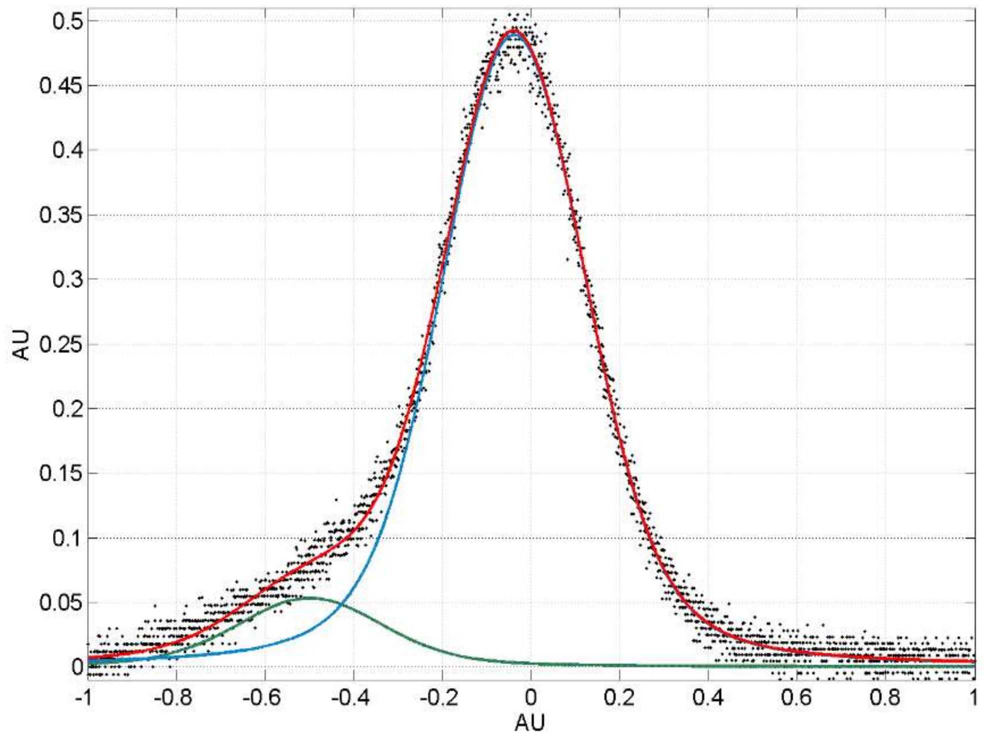

$$\mu_1 = (1.13 \pm 0.02) \cdot 10^{-4}\, s,$$
$$\mu_1 = (1.14 \pm 0.02) \cdot 10^{-4}\, s$$

$$T_{Ne} = \sqrt{\frac{\Gamma_{20}^2 * m_{20}}{\lambda \ln 2\, K_B}} \sim 360\, K$$

Stability and accuracy improvement

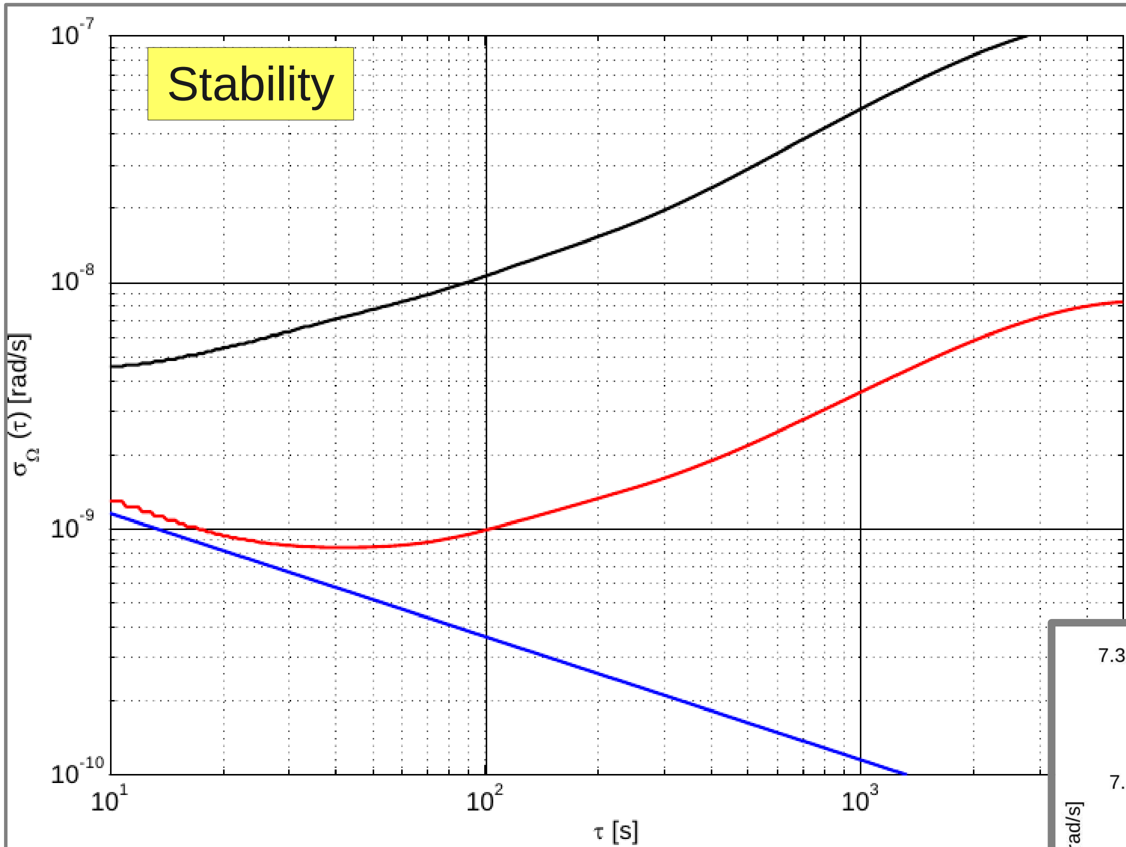

2 days of acquisition
in a noisy environment

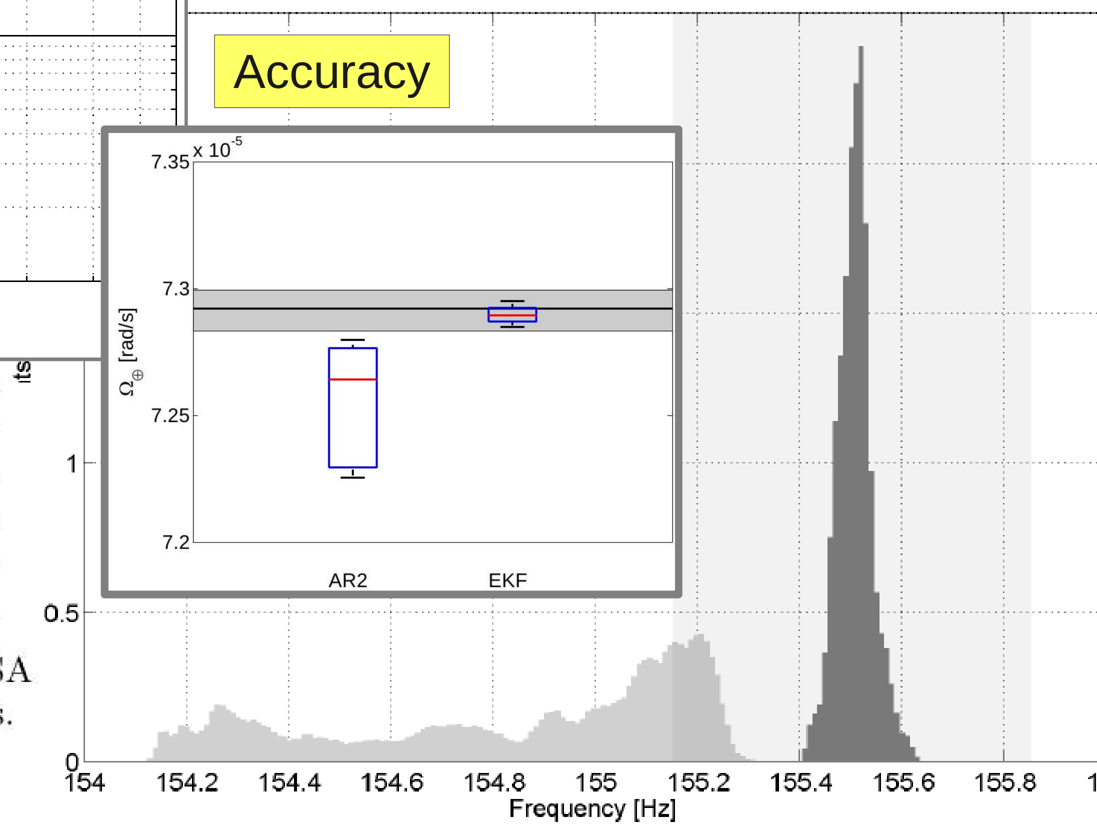

Error Source	Freq. error
Back-scattering $\mathcal{R}_2 e^{-X} + \mathcal{R}_1 e^{X} +$ c.c.	0.4695 Hz
Null Shift $\tau\,(I_1 - I_2)$	-8.7×10^{-4} Hz
Atomic Scale Factor $\sigma_1 - \sigma_2$	5.56×10^{-6} Hz
Cross Dispersion $I\,(\tau_{21} - \tau_{12})$	1.75×10^{-6} Hz

TABLE II: Contributions to the accuracy budget of G-PISA from systematic errors in the estimate of Lamb parameters.

D. Cuccato et. al, arXiv:1309.4694v1

Conclusions & Perspectives

The mid-size RLG "G-Pisa" can find application for:
-Ground tilt monitoring of special environements (GW detetctors)

-In-situ rotational seismology (orientability+transportability)

-Active controls development and characterization

Present activity:
-Strategy for the geometry control (Diagonals+Perimeter)

-Estimation of the laser-dynamics effects on the rotation measurement (stability and accuracy)

Future activity:
-Implement **full geometry control** (diagonals+perimeter) on GP-2 (Pisa).

-Test the Kalman filter on the data of **"G" (Wettzell)**.

-Investigation of the **GranSasso environment** with a larger ring laser (Geosensor design, **L>3.5 m**) (within 2013)

Thank you for your attention!